Molecular Phylogenetics and Evolution 128 (2018) 123–146

Contents lists available at ScienceDirect

Molecular Phylogenetics and Evolution

journal homepage: www.elsevier.com/locate/ympev

Molecular phylogeny of *Ischnocnema* (Anura: Brachycephalidae) with the redefinition of its series and the description of two new species

Pedro P.G. Taucce[a,*], Clarissa Canedo[b,f], Júlia Soares Parreiras[c], Leandro O. Drummond[d], Paulo Nogueira-Costa[e,f], Célio F.B. Haddad[a]

[a] Instituto de Biociências, UNESP – Univ Estadual Paulista, Câmpus Rio Claro, Departamento de Zoologia e Centro de Aquicultura (CAUNESP), Cx. Postal 199, 13506-569 Rio Claro, SP, Brazil
[b] Instituto de Biologia Roberto Alcântara Gomes, UERJ – Universidade do Estado do Rio de Janeiro, Departamento de Zoologia, Laboratório de Diversidade e Evolução de Anfíbios, Rua São Francisco Xavier, 524, Maracanã, 20550-013 Rio de Janeiro, RJ, Brazil
[c] Instituto de Ciências Biológicas, UFMG – Universidade Federal de Minas Gerais, Departamento de Zoologia, Laboratório de Herpetologia, Avenida Antônio Carlos, 6627, Pampulha, 31270-910 Belo Horizonte, MG, Brazil
[d] Universidade Federal do Rio de Janeiro (UFRJ), Departamento de Ecologia, Laboratório de Vertebrados, Cx. Postal 68020, Ilha do Fundão, CEP 21941-901 Rio de Janeiro, RJ, Brazil
[e] Instituto de Biologia Roberto Alcântara Gomes, UERJ – Universidade do Estado do Rio de Janeiro, Departamento de Ecologia, Laboratório de Ecologia de Vertebrados, Rua São Francisco Xavier, 524, Maracanã, 20550-013 Rio de Janeiro, RJ, Brazil
[f] Universidade Federal do Rio de Janeiro, Museu Nacional, Departamento de Vertebrados, Quinta da Boa Vista, s/n, 20940-040 Rio de Janeiro, RJ, Brazil

ARTICLE INFO

Keywords:
Amphibia
Bioacoustics
Brachycephaloidea
Systematics
Taxonomy
Terrarana

ABSTRACT

We present a new phylogenetic hypothesis for *Ischnocnema*, a Neotropical brachycephaloid genus of ground-dwelling direct-developing frogs. We performed Bayesian inference, maximum likelihood, and maximum parsimony analyses using two nuclear (*RAG1* and *Tyr*) and three mitochondrial genes (12S rRNA, tRNA-Val, and 16S rRNA) in a matrix comprising more than 80% of the described species. We recover *Ischnocnema nanahallux* outside the *Ischnocnema parva* series, and it is now unassigned to any species series, nor are *Ischnocnema manezinho* and *Ischnocnema sambaqui*. We propose the *Ischnocnema venancioi* species series to comprise *Ischnocnema venancioi*, *Ischnocnema hoehnei*, and two new species described herein (*Ischnocnema parnaso* sp. nov. and *Ischnocnema colibri* sp. nov.). Furthermore, we designate a lectotype for *I. venancioi*. The nuptial pad present in males is an important character in the genus, and having a large, conspicuous, and glandular-appearing nuptial pad seems to be a synapomorphy for the clade composed of the *I. parva*, *Ischnocnema guentheri*, and the newly proposed *I. venancioi* series.

1. Introduction

The Neotropical genus *Ischnocnema* Reinhardt and Lütken, 1862, is a group of ground-dwelling frogs belonging to Brachycephaloidea Günther, 1858, a superfamily of direct-developing frogs (*i.e.*, they do not go through a larval phase during their development). It currently comprises 35 species (Frost, 2018) divided into four series distributed throughout South and Southeast Brazil and adjacent Argentina, mainly in the Atlantic Forest domain: *Ischnocnema guentheri*, *Ischnocnema lactea*, *Ischnocnema parva*, and *Ischnocnema verrucosa* (Canedo and Haddad, 2012; Padial et al., 2014). Not long ago *Ischnocnema* was considered a junior synonym of *Eleutherodactylus* Dumeril and Bibron, 1841 (Caramaschi and Canedo, 2006), but the taxonomic status of the genus and its species has changed.

Lynch (1976) divided the South American *Eleutherodactylus* into ten groups, based on morphological characters. Four of these groups contained species from the Atlantic Forest: the *E. binotatus* group, which included *Eleutherodactylus binotatus* (Spix, 1824), *Eleutherodactylus gualteri* B. Lutz, 1974, *Eleutherodactylus guentheri* (Steindachner, 1864), *Eleutherodactylus nasutus* (A. Lutz, 1925), *Eleutherodactylus octavioi* Bokermann, 1965, and *Eleutherodactylus plicifer* (Boulenger, 1888); the *E. lacteus* group, which included *Eleutherodactylus bolbodactylus* (A. Lutz, 1925), *Eleutherodactylus lacteus* (Miranda-Ribeiro, 1923), *Eleutherodactylus nigriventris* (A. Lutz, 1925), and *Eleutherodactylus venancioi* B. Lutz, 1958; the *E. parvus* group, which included *Eleutherodactylus parvus* (Girard, 1853) and *Eleutherodactylus pusillus* Bokermann, 1967; and finally the *Eleutherodactylus ramagii* group, which included *Eleutherodactylus paulodutrai* Bokermann, 1975 and *Eleutherodactylus*

* Corresponding author.
E-mail address: pedrotaucce@gmail.com (P.P.G. Taucce).

https://doi.org/10.1016/j.ympev.2018.06.042
Received 10 April 2018; Received in revised form 26 June 2018; Accepted 27 June 2018
Available online 02 July 2018

ramagii (Boulenger, 1888).

Heyer (1984) created the *E. guentheri* cluster to comprise part of the *E. binotatus* group and three new species that he described at the time. The cluster contained *Eleutherodactylus epipedus* Heyer, 1984, *Eleutherodactylus erythromerus*, Heyer, 1984, *E. gualteri*, *E. guentheri*, *E. nasutus*, and *Eleutherodactylus oeus* Heyer, 1984.

Further, Lynch and Duellman (1997) created the *E. binotatus* series to comprise the four Atlantic Forest groups from Lynch (1976). To the *E. binotatus* group (*sensu* Heyer, 1984) the authors added *Eleutherodactylus heterodactylus* (Miranda-Ribeiro, 1937), *Eleutherodactylus hoehnei* B. Lutz, 1958, *Eleutherodactylus izecksohni* Caramaschi and Kisteumacher, 1989, and *Eleutherodactylus juipoca* Sazima and Cardoso, 1978. From the *E. lacteus* group, the authors removed *E. venancioi* and included *Eleutherodactylus holti* Cochran, 1948, while the *E. parvus* and *E. ramagii* groups remained the same. The authors also assigned *Eleutherodactylus randorum* Heyer, 1985; *Eleutherodactylus spanios* Heyer, 1985; *E. venancioi*; and *Eleutherodactylus vinhai* Bokermann, 1975 to the *E. binotatus* series, despite not having been assigned to any group.

Until recently, the genus *Ischnocnema* contained only one member from the Atlantic Forest, *Ischnocnema verrucosa* (Reinhardt and Lütken, 1862) while the other six species were from the Andes and their vicinities (Padial et al., 2005). Caramaschi and Canedo (2006), based on osteological features observed in *I. verrucosa* (type species of the genus), placed *Ischnocnema* under the synonymy of *Eleutherodactylus* (where most current brachycephaloid frogs were placed at the time) and resurrected *Oreobates* Jiménez de la Espada, 1872, to comprise the five Andean species. Heinicke et al. (2007) then resurrected *Ischnocnema* to comprise the *Eleutherodactylus* from the Brazilian Atlantic Forest, with the exception of the former *E. binotatus* and *E. plicifer*, currently placed in the genus *Haddadus* Hedges, Duellman, and Heinicke, 2008. Hedges et al. (2008) presented a phylogenetic hypothesis and proposed a new classification for New World direct-developing frogs, a clade they called Terrarana (currently the superfamily Brachycephaloidea). Although only a few *Ischnocnema* species were present in their phylogenetic hypothesis (five of 29 species at the time), they divided the genus into five species series based on morphology and previous taxonomic proposals: *I. guentheri*, *I. lactea*, *I. parva*, *Ischnocnema ramagii*, and *I. verrucosa*. The *I. guentheri* series contained the species from Heyer (1984) plus *Ischnocnema henselii* (Peters, 1870), which was resurrected from the synonymy of *I. guentheri* by Kwet and Solé (2005), and *Ischnocnema hoehnei*, *Ischnocnema octavioi*, *Ischnocnema izecksohni*, and *Ischnocnema vinhai*. The *I. lactea* series contained the species from the *E. lacteus* group from Lynch and Duellman (1997) plus *Ischnocnema bilineata* (Bokermann, 1975), *Ischnocnema gehrti* (Miranda-Ribeiro, 1926), *Ischnocnema manezinho* (Garcia, 1996), *Ischnocnema paranaensis* (Langone and Segalla, 1996), *Ischnocnema randorum*, *Ischnocnema sambaqui* (Castanho and Haddad, 2000), *Ischnocnema spanios*, and *Ischnocnema venancioi*. The *I. parva* and *I. ramagii* series had the same content as the *E. parvus* and *E. ramagii* groups of Lynch and Duellman (1997), respectively. Hedges et al. (2008) also created the *I. verrucosa* series to comprise *I. verrucosa* and *Ischnocnema juipoca*.

Canedo et al. (2010) described *Ischnocnema surda* Canedo, Pimenta, Leite, and Caramaschi, 2010, and placed it in the *I. verrucosa* series. They also took *I. octavioi* out of the *I. guentheri* series and placed it, together with *Ischnocnema penaxavantinho* Giaretta, Toffoli, and Oliveira, 2007, in the *I. verrucosa* series based on morphological characters. Canedo and Haddad (2012) proposed a new classification for the superfamily Brachycephaloidea based on the greatest sampling of *Ischnocnema* in a phylogenetic study until then, with about 80% of its described species. Among their most important findings was that the *I. ramagii* series and *I. vinhai* actually belonged to *Pristimantis* Jiménez de la Espada, 1870, and that *I. bilineata* was part of a distinct family of Brachycephaloidea, Craugastoridae Hedges, Duellman, and Heinicke, 2008. Because they could not precisely identify the generic relationships of the latter, they placed it as *incertae sedis* within the subfamily Holoadeninae Hedges, Duellman, and Heinicke, 2008. They also changed the content of all remaining *Ischnocnema* species series (except for *I. parva*), with most of the changes occurring in the *I. lactea* series. *Ischnocnema abdita* Canedo and Pimenta, 2010 (placed in the *I. lactea* series based on morphology in the original description) and *Ischnocnema bolbodactyla* were assigned to the *I. verrucosa* series, and *I. venancioi* went to the *I. guentheri* series. Additionally, Canedo and Haddad (2012) removed *I. manezinho* and *I. sambaqui* from the *I. lactea* series, and did not place them in any other series because of ambiguity in the phylogenetic position of the clade composed of these species. The recently described *Ischnocnema concolor* Targino, Costa, and Carvalho-e-Silva, 2009, *Ischnocnema melanopygia* Targino, Costa, and Carvalho-e-Silva, 2009, and *Ischnocnema vizzotoi* Martins and Haddad, 2010, had their taxonomic position confirmed within the *I. lactea* series. Later, the *I. parva* series gained a third member with the description of *Ischnocnema nanahallux* Brusquetti, Thomé, Canedo, Condez, and Haddad, 2013. Brusquetti et al. (2013) proposed a phylogenetic hypothesis including only five species of *Ischnocnema* and one *Brachycephalus* Fitzinger, 1826, where *I. nanahallux* was the sister species of *I. parva*. Despite many morphological similarities between *I. nanahallux* and the other members of the *I. parva* series, Taucce et al. (2018) tested its phylogenetic position in a more comprehensive matrix, including all species of *Ischnocnema* with available genetic data at the time, and recovered it within the *I. parva* without resolution. They argued that this lack of support was probably because they only had about 500 bp available for *I. nanahallux*, while their final alignment had more than 3500 bp. These authors also described *Ischnocnema feioi* Taucce, Canedo, and Haddad, 2018, and *Ischnocnema garciai* Taucce, Canedo, and Haddad, 2018, and placed them within the *I. guentheri* series.

Recent fieldwork and museum visits allowed us to discover new populations of *Ischnocnema* morphologically similar to *I. hoehnei* and *I. venancioi*, in the Brazilian states of Rio de Janeiro and Espírito Santo and to improve the gene sampling of *I. nanahallux*. Our main goals with this paper are to: (1) construct a robust molecular phylogenetic hypothesis for *Ischnocnema* with a better sampling than previous papers to improve the resolution of the *I. guentheri* and *I. parva* species series, the phylogenetic position of *I. nanahallux* and to assess the position of our new populations, and (2) evaluate, using three lines of evidence (molecular, acoustic, and morphological data), whether our newly discovered populations are conspecifics to *I. hoehnei* and *I. venancioi* or distinct evolving lineages deserving a name.

2. Material and methods

2.1. Taxon and gene sampling

We compiled a molecular dataset with an ingroup composed of all available *Ischnocnema* species in GenBank (all terminals and respective accession numbers, including those sequences produced during this work, are listed in Appendix A). Species we were not sure about the exact identification we added the qualifier *confer* (cf.) to its name. When the species had some morphological affinity to a described species but we had some evidence (by examining the voucher or in the literature) that the species were new to science, we added the qualifier *affinis* (aff.) to its name. In order to avoid spending computational time, we tried to keep terminals at a maximum of two per species, with two exceptions. *Ischnocnema guentheri* was shown to be endemic to the Tijuca Massif, Rio de Janeiro, Brazil, and together with *I. henselii* and other candidate species to form a complex of at least six species (Gehara et al., 2013), and we used two terminals of each of these species. Gehara et al. (2017) showed *I. parva* is also a complex of several species, and we used at least one terminal of each of the lineages of the study in our phylogenetic hypotheses. We also added a species morphologically similar to *I. parva* from the municipality of Camacan, Bahia, Brazil, more than 900 km from the type locality of *I. parva* (municipality of Rio de Janeiro, Rio de Janeiro, Brazil). We checked the voucher and it has important morphological differences from *I. parva;* thus, we treat it as a

different species. Because of its lack of resolution in previous phylogenetic studies (see Taucce et al., 2018), we raised the gene sampling of *I. nanahallux*, adding two nuclear genes and two mitochondrial genes, in an attempt to improve the resolution of its phylogenetic position. We also included specimens from three putative new species related to *I. venancioi* and *I. hoehnei*: one from the municipality of Cachoeiras de Macacu, one from the high grasslands of the Serra dos Órgãos National Park (PARNASO), both from the state of Rio de Janeiro, and one from the municipality of Santa Teresa, state of Espírito Santo. We did not have tissue samples of seven *Ischnocnema* species. Four were described more than 30 years ago and were not collected at least since the late 1970's (*I. epipeda*, *I. gehrti*, *I. gualteri*, and *I. pusilla*; Heyer, 1984), and one was described more than 20 years ago (*I. paranaensis*) and is known from its type locality only. We went to the type localities of *I. epipeda*, *I. gehrti*, and *I. gualteri* (Santa Teresa, state of Espírito Santo; Paranapiacaba, municipality of Santo André, state of São Paulo; and Granja Comari, municipality of Teresópolis, state of Rio de Janeiro; Miranda-Ribeiro, 1926; Heyer, 1984), but we did not succeed in finding them. We used as outgroups six *Brachycephalus* species (previous hypothesis used only two; Canedo and Haddad, 2012; Taucce et al., 2018), to represent the other lineage within the family Brachycephalidae, and one species from each of the following brachycephaloid genera: *Bryophryne* Hedges, Duellman and Heinicke, 2008; *Craugastor* (Cope, 1862); *Eleutherodactylus*; *Haddadus*; *Hypodactylus* Hedges, Duellman, and Heinicke, 2008; *Lynchius* Hedges, Duellman, and Heinicke, 2008; *Pristimantis*; and *Yunganastes* Padial, Castroviejo-Fisher, Köhler, Domic, and de la Riva, 2007.

Supplementary data associated with this article can be found, in the online version, at https://doi.org/10.1016/j.ympev.2018.06.042.

We chose the mitochondrial 12S rRNA, tRNA Val, and partial sequence of 16S rRNA genes, and partial sequences of the nuclear genes tyrosinase precursor (*Tyr*) and recombination activation gene 1 (*RAG1*), because they have been successfully used in most of the systematic studies of the Brachycephaloidea (*e.g.* Hedges et al., 2008; Canedo and Haddad, 2012; Padial et al., 2014).

2.2. Laboratory procedures

We extracted whole DNA from 100% ethanol-preserved muscle tissue using an ammonium acetate precipitation method (adapted by Lyra et al., 2017 from Maniatis et al., 1982) and then performed PCR amplifications using Taq DNA Polymerase Master Mix (Ampliqon S/A, Denmark) and Axygen Maxygene thermocyclers. The standard PCR program for the mitochondrial markers follows Taucce et al. (2018). For the nuclear markers we used a nested-PCR program consisting of a first PCR reaction using the most external primers (Table 1). We then took 1 μL of the reaction product, added the most internal primers, and did a second PCR reaction. The first reaction consisted of a 3-min initial denaturing step at 95 °C, followed by 20 cycles of 20 s at 95 °C, 20 s at 52 °C, and 45 s at 68 °C, followed by a final extension step of 3 min at 68 °C. The second reaction consisted of a 3-min initial denaturing step at 95 °C, followed by 40 cycles of 20 s at 95 °C, 20 s at 53 °C, and 45 s at 68 °C, followed by a final extension step of 3 min at 68 °C. We purified PCR products following Lyra et al. (2017), which were sequenced in both directions, with a BigDye Terminator Cycle Sequencing Kit (version 3.0, Applied Biosystems) in an ABI 3730 automated DNA sequencer (Applied Biosystems) at Macrogen Inc. (Seoul, South Korea).

2.3. Molecular analyses

2.3.1. Alignment, partition schemes, and nucleotide substitution model selection

We performed alignment using MAFFT v7.130b (Katoh and Standley, 2013). For the nuclear gene fragments, we used the G-INS-i algorithm, which assumes that the entire region can be aligned. For the mitochondrial gene fragments we used the E-INS-i algorithm, which is adapted for sequences with conserved domains and rich in gaps.

We conducted an *a priori* partition scheme with the three mitochondrial gene fragments and each codon position of the nuclear fragments as separate partitions. Then we made a search for the best partition scheme and best-fitting nuclear models using PartitionFinder 2.1.1 (Lanfear et al., 2017) under the Corrected Akaike Information Criterion (AICc; Hurvich and Tsai, 1989). PartitionFinder uses maximum likelihood software to conduct part of the analyses, and we chose PhyML 3.0 (Guindon et al., 2010) for this purpose.

2.3.2. Phylogenetic analyses and genetic distances

We conducted tree searches using three optimality criteria: Bayesian inference, maximum likelihood, and maximum parsimony. We computed Bayesian inference analysis in MrBayes 3.2.6 (Ronquist et al., 2012) using two independent runs of 1.0×10^7 generations, starting with random trees and four Markov chains (one cold), sampled every 1000 generations. We discarded 25% of generations and trees as burnin and performed the run with unlinked character state frequencies, substitution rates of the GTR model, gamma shape parameters, and proportion of invariable sites between partitions. We used the standard deviation of split frequencies (< 0.01), Estimated Sample Size (ESS > 100), and Potential Scale Reduction Factor (PSRF; Gelman and Rubin, 1992; should approach 1.0 as runs converge) to assess run convergence. We computed maximum likelihood analysis in RAxML v.

Table 1
Primers used in this study.

Primer		Gene	Sequence	Reference
tRNAphe-L	F	12S	AAAGCATAACACTGAAGATGTTAAGATG	Goebel et al. (1999)
tRNAval-H	R	12S–tRNA-V	GGTGTAAGCGARAGGCTTTKGTTAAG	Goebel et al. (1999)
12SL13	F	tRNA-V–16S	TTAGAAGAGGCAAGTCGTAACATGGTA	Feller and Hedges (1998)
16STitus_1	R	16S	GGTGGCTGCTTTTAGGCC	Titus and Larson (1996)
16SL2A	F	16S	CCAAACGAGCCTAGTGATAGCTGGTT	Hedges (1994)
16S-H10	R	16S	TGCTTACGCTACCTTTGCACGGT	Hedges (1994)
16SAR	F	16S	CGCCTGTTTATCAAAAACAT	Palumbi et al. (1991)
16S-Wilk2	R	16S	GACCTGGATTACTCCGGTCTGA	Wilkinson et al. (1996)
Tyr1B[a]	F	Tyrosinase	AGGTCCTCYTRAGGAAGGAATG	Bossuyt and Milinkovitch (2000)
Tyr1E[a]	R	Tyrosinase	GAGAAGAAAGAWGCTGGGCTGAG	Bossuyt and Milinkovitch (2000)
Tyr1C[b]	F	Tyrosinase	GGCAGAGGAWCRTGCCAAGATGT	Bossuyt and Milinkovitch (2000)
Tyr1G[b]	R	Tyrosinase	TGCTGGGCRTCTCTCCARTCCCA	Bossuyt and Milinkovitch (2000)
R182[a]	F	RAG1	GCCATAACTGCTGGAGCATYAT	Heinicke et al. (2007)
R270[a]	R	RAG1	AGYAGATGTTGCCTGGGTCTTC	Heinicke et al. (2007)
RAG1FF2[b]	F	RAG1	ATGCATCRAAAATTCARCAAT	Heinicke et al. (2007)
RAG1FR2[b]	R	RAG1	CCYCCTTTRTTGATAKGGWCATA	Heinicke et al. (2007)

[a] Most external primers.
[b] Most internal primers.

8.2.10 (Stamatakis, 2014), searching the most likely tree 100 times and conducting 1000 non-parametric bootstrap replicates. We used the software TNT v. 1.5 (Goloboff and Catalano, 2016) treating gaps as missing data to construct the maximum parsimony hypothesis. The search for the most parsimonious tree was made using 50 RAS + TBR holding 100 trees per replicate, and the resulting trees were used to construct a strict consensus tree. Parsimony Jackknife absolute frequencies were estimated on the consensus tree using 50 RAS + TBR and holding 10 trees per replicate for a total of 1000 replicates. The command *ttags* was used to save a SVG version of the tree. We used *Eleutherodactylus* as the root for all analyses, and we drew the Bayesian inference tree using FigTree 1.4.2 (Rambaut, 2014).

We used the mitochondrial 16S rRNA fragment limited by the primers 16SAR and 16SBR (ca. 600 bp; Palumbi et al., 1991) to calculate genetic distances among *I. hoehnei*, *I. venancioi*, and our newly discovered populations. We estimated the uncorrected pairwise distances ignoring any positions with gaps utilizing R platform version 3.3.3 (R Core Team, 2017) with the packages APE version 5.0 (Paradis et al., 2004) and SPIDER version 1.4-2 (Brown et al., 2012).

2.3.3. Species-tree analysis and divergence times

We reconstructed a dated species tree using the fully Bayesian multispecies coalescent method StarBeast2 (Ogilvie et al., 2017) implemented in the software package BEAST v.2.5.0 (Bouckaert et al., 2014) using *Ischnocnema* terminals only. We used all terminals used in our phylogenetic analyses, except for *I. parva* from the type locality, because the available *RAG1* fragment for the species is not homologous to the one we use herein, and StarBEAST2 requires that all species have all gene fragments used in the analysis. For this reason, we also used the three mitochondrial fragments as a single partition. We explain our taxon and gene sampling, as well as our species hypotheses in Section 2.1. In order to find the best-fitting nucleotide substitution model for each partition, we used the package bModelTest (Bouckaert and Drummond, 2017). The search for the best-fitting model runs concomitantly with the BEAST v.2.5.0 and StarBEAST2 analysis.

To date our species tree we used the substitution rates of 16S rRNA gene from *I. parva* (Gehara et al., 2017), which is 0.006/site/Mya, and applied it in our mitochondrial partition. We used a broad prior with $1/x$ distribution in the nuclear fragments and the program coestimated their substitution rates. We assumed a relaxed clock model with uncorrelated lognormal distribution for the mitochondrial partition and a strict clock for both nuclear partitions, and a Yule model for the species-tree. Because of the broad priors that we used in the nuclear clock models, in order to facilitate the convergence of our parmeters we did not estimate the relative rates among partitions. We ran the MCMC chain for 100,000,000 generations, sampling every 10,000 generations, and we discarded 10% of the total samples as burn-in. We checked convergence of the parameters using TRACER, and we considered that a parameter converged when the ESS was higher than 200. We summarized the tree using Tree Annotator and visualized it using FigTree 1.4.2 (Rambaut, 2014).

2.4. Morphological analyses

We took the following measurements to the nearest 0.1 mm with a Mitutoyo® digital caliper under a stereomicroscope: snout-vent length (SVL), head length (from the tip of the snout to the angle of the jaw), head width (between the angles of the jaws), forearm length (from the elbow to the wrist), hand length (from the wrist to the tip of the third finger), thigh length (from the middle of the cloacal opening to the outer edge of the knee), tibia length (from the outer edge of the knee to the outer edge of the heel), tarsal length (from the outer edge of the heel to the inner metatarsal tubercle), and foot length (from the proximal border of the inner metatarsal tubercle to the tip of the fourth toe). We also took eye diameter (between anterior and posterior margins of the eye), tympanum diameter (between anterior and posterior margins of the tympanum), eye-nostril distance (from the anterior margin of the eye to the posterior margin of the nostril), internarial distance (between the two medial margins of the nostrils), eye-to-eye distance (between the anterior margins of the eyes), third finger disk length (maximum width of disk on third finger), and fourth toe disk length (maximum width of disk on fourth toe) with an ocular micrometer coupled to a stereomicroscope. Sex was determined by the observation of nuptial pads and vocal slits in males and direct observation of the gonads of female specimens. Morphological nomenclature follows previous literature on Brachycephaloidea (Heyer, 1984; Heyer et al., 1990; Hedges et al., 2008; Duellman and Lehr, 2009). Museum acronyms follow Sabaj (2016) and a full list of specimens examined is given in Appendix B.

2.5. Call analyses

We recorded advertisement calls using a Marantz PMD 661 or a Tascam DR-40, coupled to a Sennheiser K6/ME66 unidirectional microphone. Recordings were performed at 44.1 kHz with a 16 bit sampling size. Oliveira et al. (2008) described the call of *I. hoehnei*, and the analyzed call was kindly made available by one of the authors (Giaretta, A. A.), which we reanalyzed and redescribed to facilitate comparisons.

To analyze the recordings we used the software Raven pro 1.5 (Bioacoustics Research Program, 2011). Spectrograms were produced using a window size of 512 samples, 75% overlap, hop size of 128 samples, Discrete Fourier Transform (DFT) of 1024 samples, and window type Hann. Contrast and brightness were program default (50 points each). We obtained spectrogram and oscillogram figures using tuneR version 1.3.2 (Ligges et al., 2013) and seewave version 2.0.5 (Sueur et al., 2008) packages of R platform version 3.3.3 (R Core Team, 2017). Spectrogram figures were produced with a window length of 512 samples, 75% overlap, hop size of 128 samples, and window name Hanning. Call recordings of Pedro P. G. Taucce (PPGT 009–014) and Leandro O. Drummond (LOD 001–005) are deposited in the CFBH collection. Voucher specimens are housed at CFBH and MNRJ. We list full information for the recordings in Appendix C.

We measured the following call parameters: call duration (Köhler et al., 2017), call rise time (Hepp and Canedo, 2013), dominant frequency (Köhler et al., 2017), notes per call, note (repetition) rate (total number of notes minus one, divided by the time between the beginning of the first note to the beginning of the last note; modified from the call-rate parameter of Cocroft and Ryan (1995), and note (repetition) rate acceleration (Gehara et al., 2013). Call and note concepts follow Köhler et al. (2017).

3. Results

3.1. Molecular analyses

3.1.1. Alignment, partition schemes, and nucleotide substitution model selection

We obtained a final alignment of 3800 base pairs (bp). Mitochondrial 12S rRNA, tRNAVal, and 16S rRNA had 1029, 76, and 1528 bp respectively; nuclear *RAG1* and *Tyr* had 636 and 531 bp, respectively. Some species had one or two codon insertion-deletions in *RAG1*, and we moved them to maintain the reading frame when necessary. The best-fitting partition scheme had seven partitions, which are shown together with the respective best-fitting nucleotide substitution model in Table 2. Although we used the seven partition schemes for the maximum likelihood analysis, we used the General Time Reversible model with γ–distribution for all of them because RAxML does not support applying different models to different partitions.

3.1.2. Phylogenetic analyses and genetic distances

The maximum likelihood and Bayesian inference analyses yielded similar topologies (Fig. 1), and Bayesian inference runs converged for

Table 2
Best partition scheme and respective best fitting molecular models.

Partition	Model
12S and tVal	GTR + Γ + I
16S	GTR + Γ + I
RAG1 1st and 2nd positions	GTR + Γ
RAG1 3rd position	K80 + Γ
Tyr 1st position	GTR + Γ + I
Tyr 2nd position	HKY + Γ + I
Tyr 3rd position	GTR + Γ

following order, inside parentheses, for a clade: Bayesian inference posterior probability, maximum likelihood bootstrap, and maximum parsimony jackknife. The three topologies recovered the family Brachycephalidae (1.0, 93, and 71) and both genera *Brachycephalus* (1.0, 100, and 100) and *Ischnocnema* (1.0, 100, and 100) as monophyletic with high support, as well as the *I. lactea* (1.0, 100, and 100) and the *I. guentheri* series (0.98, 78, and 76). Within the *I. guentheri* series, the three analyses recovered *I. venancioi*, *I. hoehnei*, and our putative species in a fully supported clade (1.0, 100, and 100), separated from a clade composed of the remaining species of the *I. guentheri* series (1.0, 100,

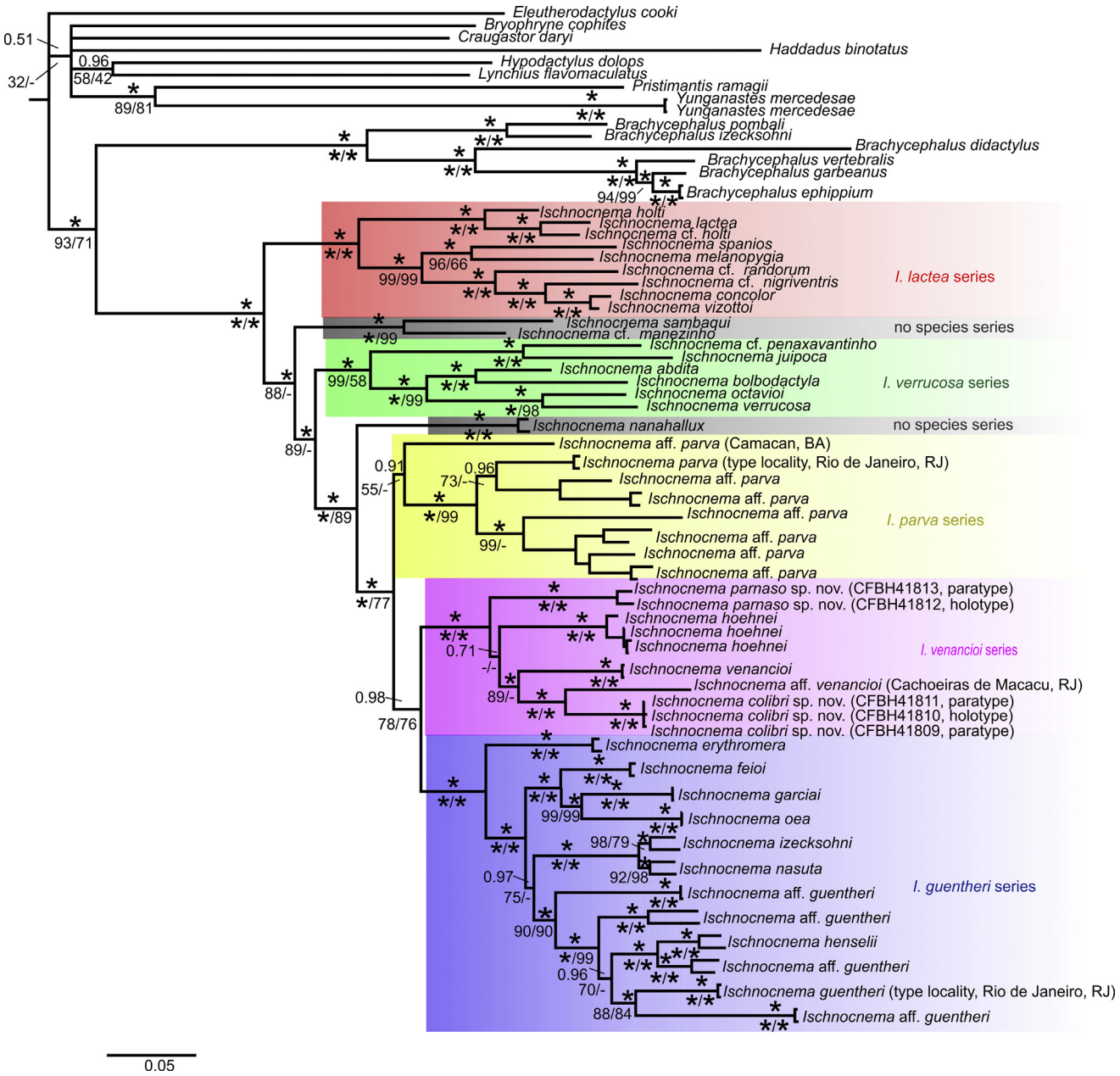

Fig. 1. The 50% majority rule consensus tree from Bayesian inference analysis of concatenated mitochondrial 12S rRNA, tVal rRNA, 16S rRNA, and nuclear Recombination Activating Gene 1 (*RAG1*) and tyrosinase precursor (*Tyr*). Posterior probabilities are shown above the branches and maximum likelihood bootstrap and parsimony jackknife are shown below the branches (to the left and to the right of the bar, respectively). Asterisks (*) indicate fully supported clades and hyphens (-) indicate that the clade does not appear in the specific phylogenetic analysis.

all parameters that we checked (see Section 2.3.2). The maximum parsimony tree also yielded an overall similar topology, but some clades showed low resolution (Fig. S1). From now on we give support in the and 100), which we now redefine as the *I. venancioi* and the *I. guentheri series* respectively. The *I. verrucosa* series was also recovered as monophyletic, but it was poorly supported in the maximum parsimony

Table 3
Uncorrected pairwise genetic distances (percentage) of mitochondrial 16S rRNA fragment (ca. 600 bp) within (highlighted in gray) and among members of the *Ischnocnema venancioi* species series. Data are shown as range (mean) where appropriate. NA = not applicable.

	Uncorrected pairwise distance between species (%)				
	I. hoehnei	*I. venancioi*	*I.* aff. *venancioi* (Cachoeiras de Macacu)	*I. colibri* sp. nov.	*I. parnaso* sp. nov.
I. hoehnei	0.0–2.2 (1.1, n = 4)				
I. venancioi	10.8–12.1 (11.8)	0.0 (n = 2)			
I. aff. *venancioi*	13.6–13.8 (12.3)	11.4	NA (n = 1)		
I. colibri sp. nov.	12.3	10.5	7.3	0.0 (n = 3)	
I. parnaso sp. nov.	10.3–12.1 (11.4)	11.4–12.3 (11.9)	14.3–14.9 (14.6)	12.3–12.5 (12.4)	2.0 (n = 2)

analysis (1.0, 99, and 58). The phylogenetic placement of the clade composed of *I.* cf. *manezinho* and *I. sambaqui* (1.0, 100, and 99) was not congruent among the three analyses. This clade was the sister group of all *Ischnocnema* except for the *I. lactea* series in the Bayesian inference and the maximum likelihood analyses (1.0 and 88); while in the maximum parsimony tree this relationship was not resolved. None of the analyses recovered the *I. parva* series as monophyletic. The recently described *I. nanahallux* was the sister lineage (1.0, 100, and 89) to a clade composed of the remaining members of the *I. parva* series and the members of the *I. guentheri* and *I. venancioi* series (1.0, 100, and 77), with high support in the three topologies.

The uncorrected pairwise distance among *I. venancioi*, *I. hoehnei*, and our putative species ranged from 7.3% (population from Cachoeiras de Macacu and population from Santa Teresa) to 14.9% (population from Cachoeiras de Macacu and population from the highland grasslands of PARNASO). The uncorrected pairwise distance within species ranged from 0.0% (*I. venancioi* and the population from Santa Teresa) to 2.2% (within *I. hoehnei*). Distances between and within species are summarized in Table 3.

3.1.3. Species-tree analysis and divergence times

The resulting best-fitting nucleotide models inferred by bModelTest were TN93 + Γ + I for the mitochondrial fragment and for *RAG1*, and HKY + Γ + I for *Tyr*. All parameters had an ESS higher than 450, except for the BMT_Rates.6 for each partition, which recovered an ESS of 56, 168, and 75 for the mitochondrial fragment and nuclear *RAG1* and *Tyr* fragments respectively. The low ESS is expected in these parameters because when low parameter models are sampled (like HKY and TN93), the higher rates will be sampled very infrequently (Bouckaert and Drummond, 2017).

StarBEAST2 recovered all *Ischnocnema* species series monophyletic with strong support, except for the *I. parva* series (Fig. 2), just like the other phylogenetic analyses. However, the relationships at the base of the tree had no resolution. Our estimates of divergence times showed that the most recent common ancestor of all *Ischnocnema* dates to 48 Mya, during the middle Eocene. The divergences of the *Ischnocnema* series span a large time frame, dating from the end of Eocene to the end of Oligocene, and the divergences within the species series date mainly to the Miocene. Very few clades date to the Pliocene, and the only divergence during the Pleistocene is the one originating *I. concolor* and *I. vizottoi*.

3.2. Morphological analyses

Both external morphology and morphometric characters were important for the recognition of *I. hoehnei*, *I. venancioi*, and our putative species. However, because only one specimen from the population from Cachoeiras de Macacu was available for us to examine, we preferred to exclude it from our morphometric analysis.

Two characters distinguish both putative species from the other species of the *I. guentheri* series: Finger I smaller than Finger II (Finger I approximately the same size as Finger II in other species) and disks of fingers III and IV large and truncated (smaller and usually rounded in other species; Fig. 3). The SVL (Table 4; Fig. 4), the pattern of the posterior surface of the thigh (Fig. 5), the relative size of Finger I compared to Finger II, and the ratios foot length/SVL, tibia length/SVL, and fourth toe disk width/third finger disk width were important for differentiating *I. venancioi*, *I. hoehnei*, and the populations from Santa Teresa and the high-elevation grasslands of PARNASO. We give detailed information about the diagnostic characters and other morphological traits in the Taxonomic Accounts section.

3.3. Call analyses

We analyzed 30 advertisement calls from 12 individuals. We had calls available for *I. hoehnei* and for the putative species from Santa Teresa and the high-elevation grasslands of the PARNASO. The advertisement calls are emitted sporadically as groups of short notes, without regular intervals between calls. The first notes have low energy, with notes increasing in energy gradually until an energy peak is reached (Fig. 6A–C). All analyzed advertisement calls are different from each other, and they are distinguished mainly by the dominant frequency, note (repetition) rate, and notes per call (Table 5). We also analyzed 19 territorial calls from two individuals from the population of Santa Teresa. The territorial and advertisement calls share a similar structure, but the first has a shorter call duration and its notes increase in energy more sharply than in the latter (Fig. 6D; Table 5).

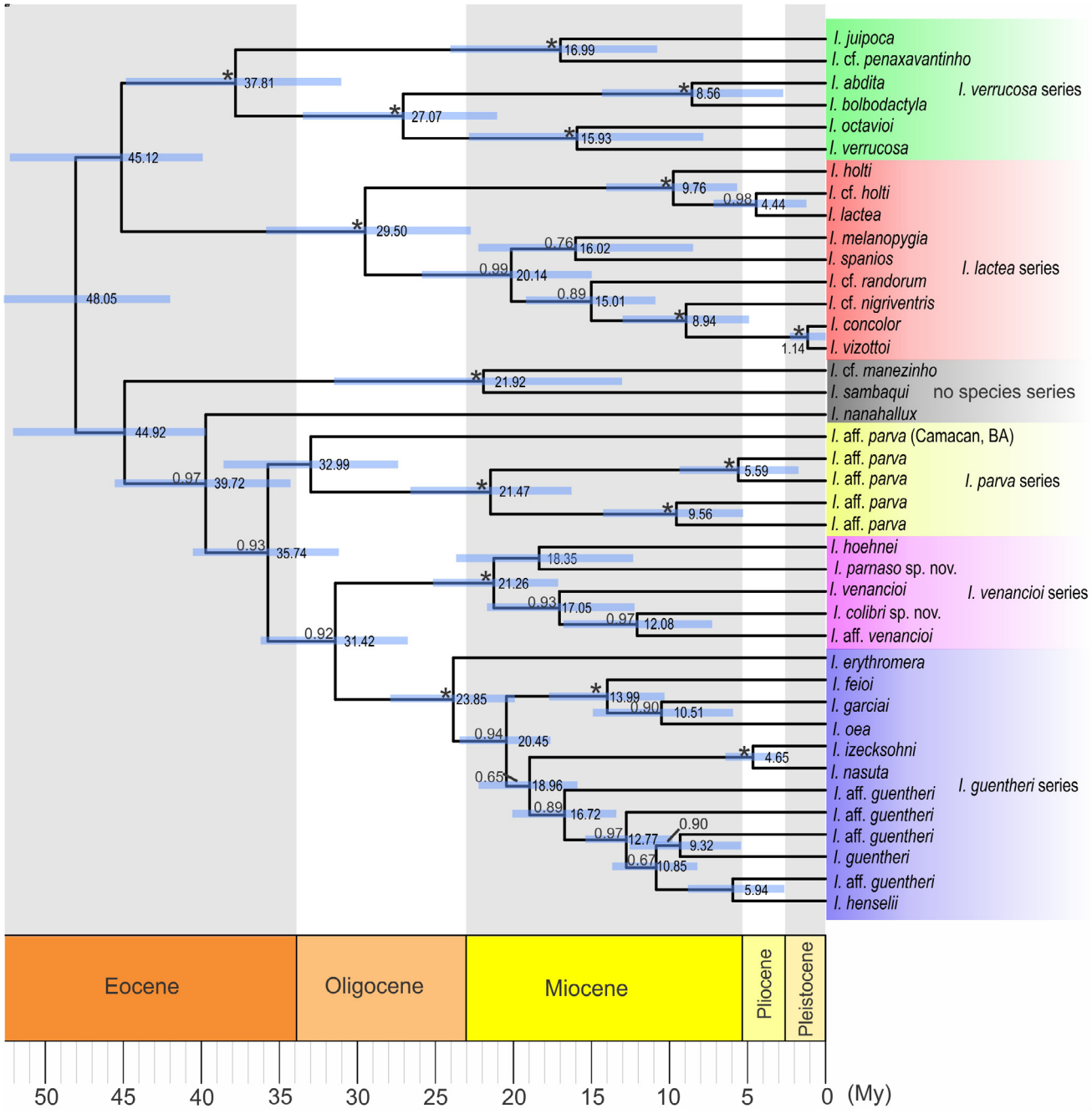

Fig. 2. Time-calibrated topology inferred from StarBEAST2 analysis. Numbers above branches indicate posterior probabilities and node numbers indicate mean node ages. Blue bars indicate standard deviation of node ages. Asterisks (*) indicate fully supported clades.

3.4. Taxonomic accounts

The *I. parva* series, as formerly known (Brusquetti et al., 2013; followed by Padial et al., 2014), comprises *I. parva*, *I. pusilla*, and *I. nanahallux*. In our three phylogenetic analyses the *I. parva* series is not recovered as monophyletic (Figs. 1 and S1), with *I. nanahallux* as the sister group of the remaining *I. parva*, *I. venancioi*, and *I. guentheri* series. So, to avoid non-monophyletic groupings, we propose the removal of *I. nanahallux* from the *I. parva* series.

Ischnocnema venancioi and *I. hoehnei* are formerly in the *I. guentheri* series (Canedo and Haddad, 2012; Padial et al., 2014; Taucce et al., 2018). We recovered these and the other related species in a fully supported clade (1.0, 100, and 100), the sister group to all the remaining members of the *I. guentheri* series. Our results show that the members of the *I. venancioi* clade, besides being molecularly different, are also phenotypically distinguishable from all other currently recognized *Ischnocnema* species series. For this reason, we propose the *I. venancioi* species series to include the members of this clade. We also redefine the *I. guentheri* series to fit this new arrangement.

Finally, based on the molecular, acoustic, and morphological evidences presented here, we consider *I. venancioi*, *I. hoehnei*, and the two populations from the high-elevation grasslands of the PARNASO and Santa Teresa as distinct evolving lineages. We also have strong molecular evidence that the population from Cachoeiras de Macacu is a distinct evolving lineage. However, because we are using an integrative approach and our only specimen from this population has no recorded advertisement call, we do not describe it as new species. The original descriptions of *I. venancioi* and *I. hoehnei* are good and were made with

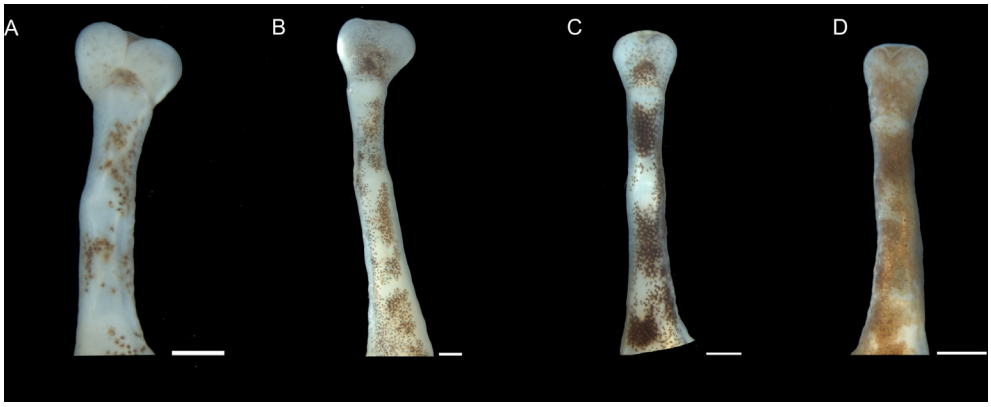

Fig. 3. Character states of the tip of Finger III in the members of the *Ischnocnema venancioi* and *I. guentheri* series: large and truncated in (A) *I. hoehnei* and (B) *I. venancioi*; rounded in (C) *I. guentheri* and (D) *I. oea*. Scale bars = 1 mm (A, C) and 0.5 mm (B, D).

care at the time (Lutz, 1958), but to bring the descriptions to a modern context and to enhance comparisons, we redescribe both species. We then describe the populations from Santa Teresa and from the high-elevation grasslands of PARNASO as new species, since there is no available name for them.

This published work and the nomenclatural acts it contains have been registered in ZooBank, the online registration system for the ICZN. The LSID (Life Science Identifier) for this publication is FA39CA94-8829-4457-8D58-D1FD8B24D47A.

3.4.1. *Ischnocnema guentheri* species series

Diagnosis: The *I. guentheri* series is distinguished from all other *Ischnocnema* species series by the following combination of characters: (1) Finger I approximately the same size as Finger II; (2) tips of fingers

Table 4
Snout-vent length (SVL) and body proportions of *Ischnocnema venancioi*, *I. hoehnei*, *I. parnaso* sp. nov., and *I. colibri* sp. nov. Data are given as range (mean ± standard deviation) where appropriate. All measurements are in millimeters.

SVL and body proportions	Adult males				Adult females			
	I. venancioi (n = 31)	*I. hoehnei* (n = 3)	*I. parnaso* sp. nov. (n = 5)	*I. colibri* sp. nov. (n = 5)	*I. venancioi* (n = 1)	*I. hoehnei* (n = 1)	*I. parnaso* sp. nov. (n = 1)	*I. colibri* sp. nov. (n = 3)
SVL	15.7–22.3 (17.5 ± 1.3)	30.6–34.8 (32.4 ± 2.2)	27.1–30.3 (28.8 ± 1.2)	22.9–25.2 (23.9 ± 1.1)	24.1	42.7	38.0	31.1–34.6 (33.3 ± 1.9)
Head length/SVL	0.37–0.47 (0.43 ± 0.03)	0.39–0.43 (0.41 ± 0.02)	0.39–0.40 (0.39 ± 0.01)	0.39–0.42 (0.40 ± 0.01)	0.40	0.43	0.39	0.41–0.43 (0.42 ± 0.01)
Head width/SVL	0.31–0.38 (0.35 ± 0.02)	0.33–0.36 (0.34 ± 0.02)	0.30–0.35 (0.34 ± 0.02)	0.32–0.35 (0.33 ± 0.1)	0.33	0.36	0.33	0.33–0.37 (0.35 ± 0.02)
Head width/head length	0.72–0.93 (0.81 ± 0.05)	0.81–0.84 (0.83 ± 0.02)	0.78–0.90 (0.86 ± 0.05)	0.79–0.82 (0.81 ± 0.01)	0.81	0.82	0.86	0.81–0.84 (0.83 ± 0.02)
Eye diameter/head length	0.26–0.36 (0.32 ± 0.02)	0.28–0.32 (0.30 ± 0.02)	0.29–0.31 (0.31 ± 0.01)	0.29–0.36 (0.32 ± 0.03)	0.23	0.34	0.25	0.26–0.29 (0.27 ± 0.01)
Tympanum diameter/ head length	0.09–0.17 (0.12 ± 0.02)	0.11–0.13 (0.12 ± 0.01)	0.10–0.13 (0.12 ± 0.01)	0.12–0.14 (0.13 ± 0.01)	0.09	0.13	0.11	0.11–0.13 (0.12 ± 0.01)
Tympanum diameter/ eye diameter	0.27–0.57 (0.37 ± 0.06)	0.40–0.43 (0.41 ± 0.01)	0.34–0.43 (0.39 ± 0.04)	0.34–0.48 (0.41 ± 0.05)	0.32	0.38	0.44	0.38–0.48 (0.43 ± 0.05)
Internarial distance/ head length	0.21–0.54 (0.43 ± 0.09)	0.29–0.32 (0.30 ± 0.02)	0.34–0.49 (0.44 ± 0.07)	0.41–0.48 (0.46 ± 0.03)	0.20	0.35	0.32	0.32–0.34 (0.33 ± 0.01)
Eye-to-eye distance/ head length	0.34–0.55 (0.46 ± 0.05)	0.57–0.59 (0.58 ± 0.01)	0.41–0.47 (0.44 ± 0.02)	0.42–0.52 (0.47 ± 0.04)	0.39	0.39	0.46	0.42–0.47 (0.44 ± 0.02)
Eye-nostril distance/ head length	0.14–0.29 (0.20 ± 0.04)	0.27–0.31 (0.29 ± 0.02)	0.19–0.30 (0.23 ± 0.04)	0.21–0.29 (0.27 ± 0.04)	0.23	0.34	0.22	0.29–0.31 (0.30 ± 0.01)
Forearm length/SVL	0.16–0.24 (0.21 ± 0.02)	0.18–0.20 (0.20 ± 0.01)	0.17–0.20 (0.19 ± 0.01)	0.18–0.21 (0.20 ± 0.01)	0.22	0.22	0.19	0.20–0.23 (0.21 ± 0.01)
Hand length/SVL	0.23–0.30 (0.26 ± 0.02)	0.31–0.32 (0.32 ± 0.01)	0.27–0.30 (0.29 ± 0.01)	0.28–0.32 (0.30 ± 0.02)	0.27	0.43	0.27	0.28–0.31 (0.29 ± 0.01)
Third finger disk width/hand length	0.12–0.24 (0.17 ± 0.03)	0.17–0.18 (0.17 ± 0.00)	0.15–0.16 (0.16 ± 0.01)	0.16–0.18 (0.17 ± 0.01)	0.20	0.18	0.16	0.16–0.19 (0.17 ± 0.01)
Fourth toe disk width/ third finger disk width	0.95–0.96 (0.96 ± 0.00)	0.53–0.93 (0.73 ± 0.12)	1.00–1.07 (1.04 ± 0.04)	0.87–0.96 (0.90 ± 0.04)	0.77	0.93	1.09	0.73–0.92 (0.84 ± 0.09)
Thigh length/SVL	0.42–0.57 (0.48 ± 0.04)	0.57–0.61 (0.59 ± 0.02)	0.51–0.55 (0.53 ± 0.01)	0.52–0.54 (0.52 ± 0.01)	0.50	0.59	0.52	0.53–0.57 (0.55 ± 0.02)
Tibia length/SVL	0.48–0.60 (0.55 ± 0.03)	0.67–0.72 (0.69 ± 0.03)	0.55–0.59 (0.58 ± 0.02)	0.56–0.59 (0.58 ± 0.01)	0.55	0.73	0.57	0.58–0.62 (0.61 ± 0.02)
Tarsal length/SVL	0.26–0.36 (0.32 ± 0.03)	0.30–0.35 (0.33 ± 0.02)	0.26–0.30 (0.28 ± 0.02)	0.27–0.30 (0.29 ± 0.01)	0.29	0.34	0.32	0.29–0.31 (0.30–0.01)
Foot length/SVL	0.40–0.54 (0.46 ± 0.04)	0.67–0.70 (0.68 ± 0.02)	0.55–0.63 (0.59 ± 0.03)	0.52–0.55 (0.53 ± 0.01)	0.48	0.67	0.62	0.54–0.60 (0.57–0.03)

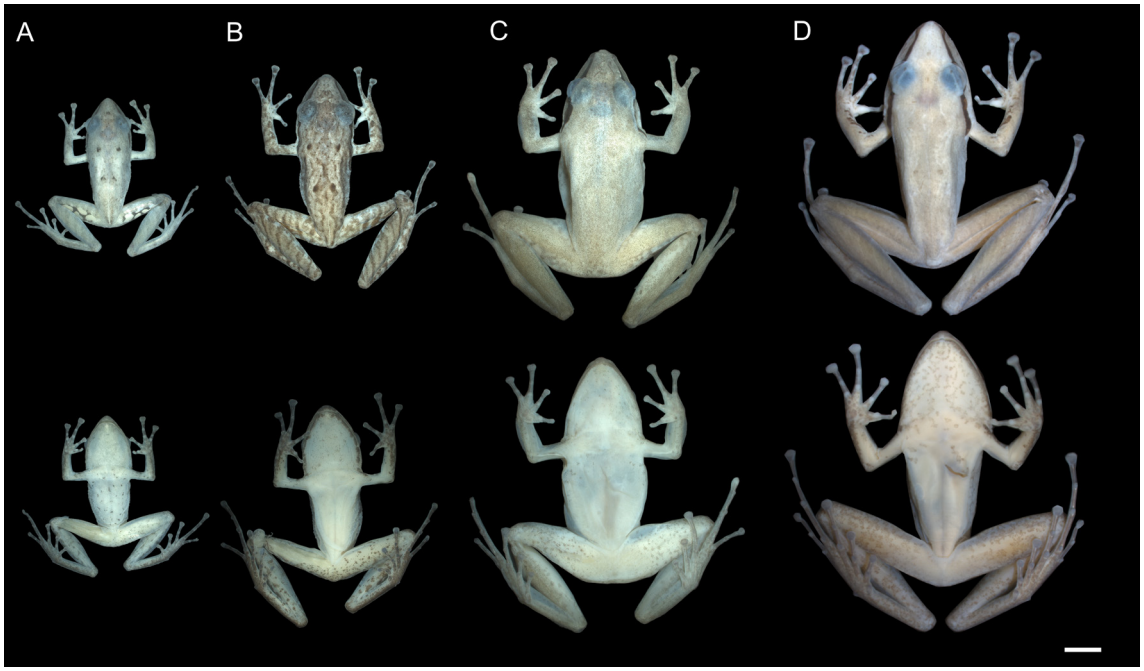

Fig. 4. Dorsal (above) and ventral (below) views of the members of the *Ischnocnema venancioi* series, showing the size differences among them: (A) *I. venancioi*, (B) *I. colibri* sp. nov., (C) *I. parnaso* sp. nov., and (D) *I. hoehnei.* Scale bar = 5 mm.

II–IV expanded, discs of fingers III and IV medium-sized and usually rounded (Fig. 3C and D); (3) long legs, tibia length > 60% of SVL; (4) one large, conspicuous, glandular-appearing nuptial pad on Finger I; (5) dorsum smooth or finely tuberculate.

Content: The taxon contains 10 species: *Ischnocnema epipeda* (Heyer, 1984); *Ischnocnema erythromera* (Heyer, 1984); *I. feioi* (Taucce, Canedo, and Haddad, 2018; *I. garciai* Taucce, Canedo, and Haddad, 2018; *Ischnocnema gualteri* (B. Lutz, 1974); *I. guentheri* (Steindachner, 1864); *I. henselii* (Peters, 1870); *I. izecksohni* (Caramaschi and Kisteumacher, 1989); *I. nasuta* (A. Lutz, 1925); and *Ischnocnema oea* (Heyer, 1984).

Distribution: The taxon is distributed throughout the Atlantic Forest in Southeast and South Brazil, in the states of Rio Grande do Sul, Santa Catarina, Paraná, São Paulo, Rio de Janeiro, Minas Gerais, and Espírito Santo. *Ischnocnema henselii* reaches the province of Misiones, northern Argentina.

Remarks: *Ischnocnema epipeda* and *I. gualteri* have yet to be phylogenetically tested, but we agree with previous authors (Canedo and Haddad, 2012; Taucce et al., 2018) and maintain these two species in the *I. guentheri* series based on external morphology. Efforts towards finding both species are of paramount importance to understand the

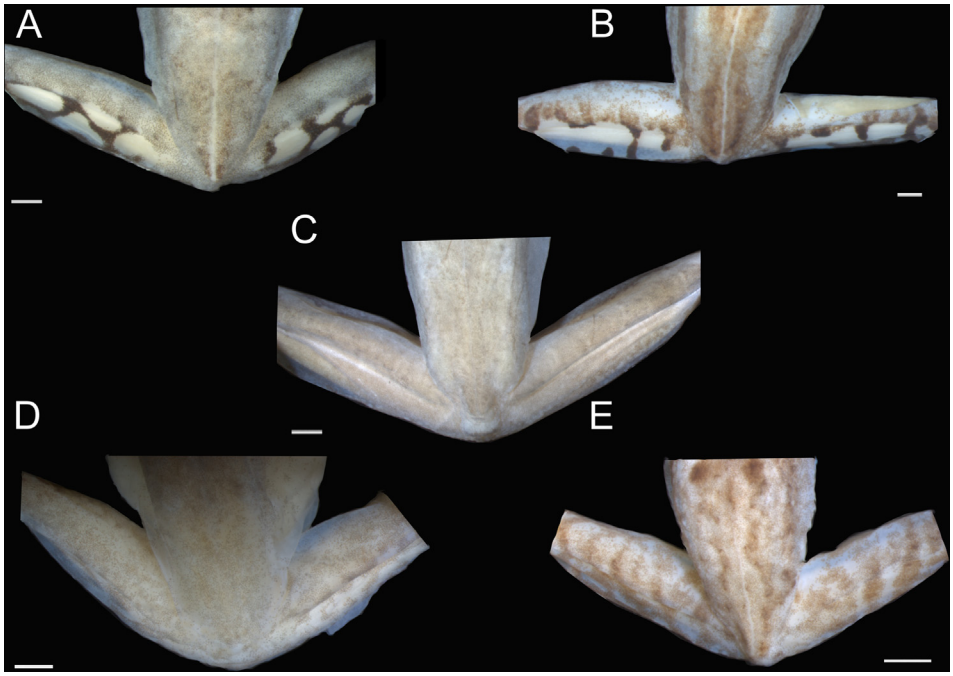

Fig. 5. Color patterns of the posterior surface of the thigh of the members of the *Ischnocnema venancioi* series: (A) and (B) *I. venancioi*, (C) *I. hoehnei*, (D) *I. parnaso* sp. nov., and (E) *I. colibri* sp. nov. Scale bar = 1 mm (A, B) and 2 mm (C–E).

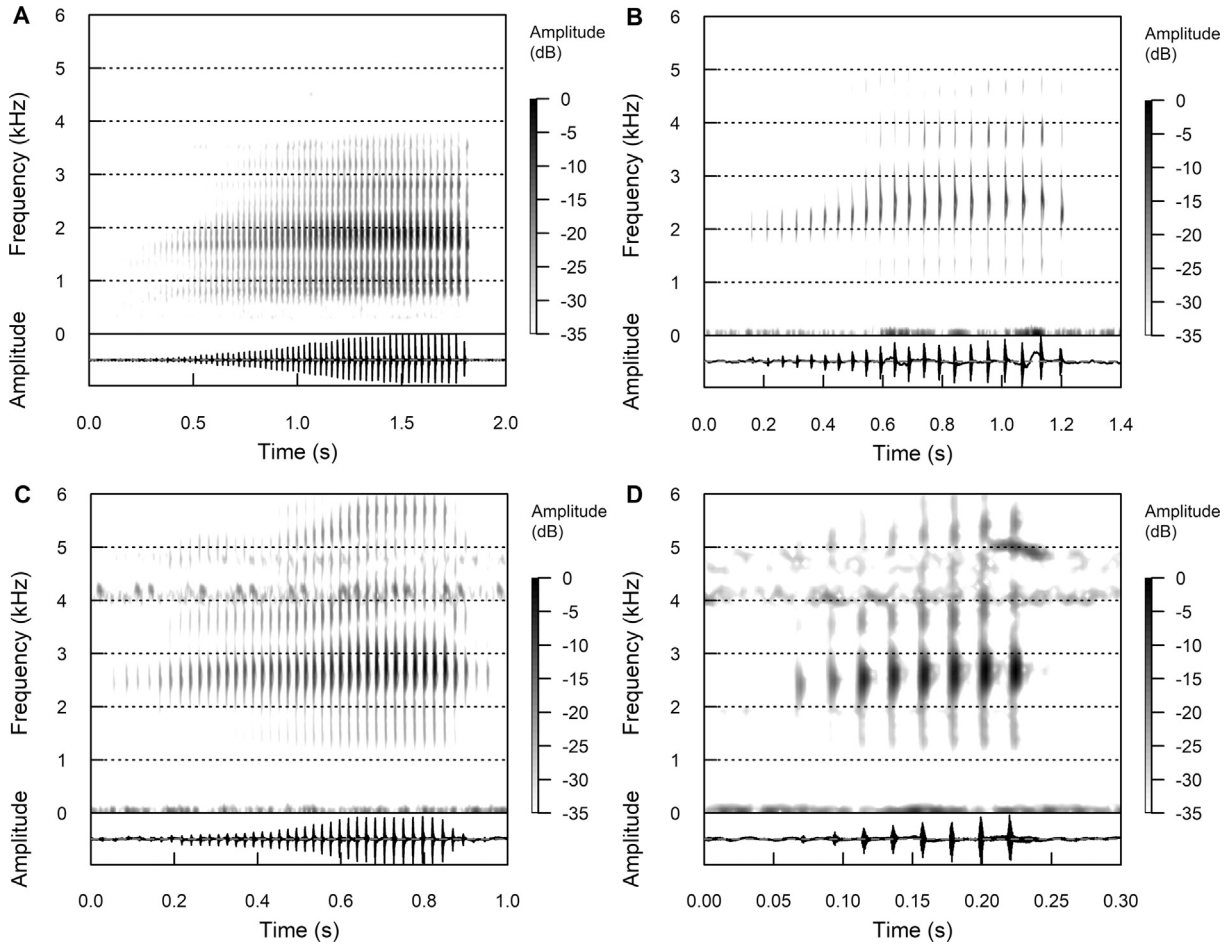

Fig. 6. Advertisement (A, B, and C) and territorial (D) calls of the members of the *Ischnocnema venancioi* series: (A) *I. hoehnei* (recording from A. A. Giaretta), (B) *I. parnaso* sp. nov. (LOD 003), and (C, D) *I. colibri* sp. nov. (PPGT 014).

phylogenetic relationships within the *I. guentheri* series.

3.4.2. *Ischnocnema venancioi* species series, new taxon

Diagnosis: The *I. venancioi* series is distinguished from all other *Ischnocnema* species series by the following combination of characters: (1) Finger I smaller than Finger II; (2) tips of fingers II–IV expanded, discs of fingers III and IV large and truncated (Fig. 3A and B); (3) one large, conspicuous, glandular-appearing nuptial pad on Finger I; (4) dark-brown to black mask-like stripe starting at the tip of the snout or the nostril, contouring the *canthus rostralis*, passing through the eye (better seen in life, color fades in preservative, Fig. 7), contouring the dorsal portion of the tympanum, and finishing near arm insertion; (5) dorsum smooth or finely tuberculate.

Content: The taxon contains four species: *I. venancioi* (Lutz, 1958), *I. hoehnei* (Lutz, 1958), *I. parnaso* sp. nov., and *I. colibri* sp. nov.

Distribution: The taxon is distributed in the mountainous lands of Serra do Mar mountain range of the states of São Paulo and Rio de Janeiro and in the north portion of the Serra da Mantiqueira mountain range in the state of Espírito Santo, all in Southeast Brazil, from 800 m to almost 2200 m of elevation (Fig. 8).

Remarks: Lutz (1958) had already grouped the species of this series, and described *I. venancioi* and *I. hoehnei* in the same paper. All subsequent phylogenetic hypotheses including both species have recovered them as sister taxa (Canedo and Haddad, 2012; Taucce et al., 2018). The two species were previously placed in the *I. guentheri* series (Canedo and Haddad, 2012; Padial et al., 2014; Taucce et al., 2018), and despite the two series being always recovered as sister taxa (Canedo and Haddad, 2012; Taucce et al., 2018, this study), the previously proposed morphological diagnosis for the *I. guentheri* series, including the *I. venancioi* series members, is no longer applicable for species of both series together. We recovered the *I. venancioi* series as a fully-supported clade in our three analyses, and our data show that these species share some

Table 5
Acoustic parameters comparing the advertisement calls of the members of the *Ischnocnema venancioi* species series and the territorial call of *I. colibri* sp. nov. Data are given as ranges when applicable.

Species	*I. hoehnei*	*I. parnaso* sp. nov.	*I. colibri* sp. nov.	
Type of call	Advertisement call	Advertisement call	Advertisement call	Territorial call
Call duration (s)	1.65	1–1.5	0.9–1.2	0.17–0.51
Call rise time (%)	96	42–92	53–89	5–92
Dominant frequency (kHz)	1.9	2.34–2.67	2.67–2.84	2.63–2.93
Notes per call	59	18–29	40–53	8–23
Note rate (notes/s)	35.78	16.55–21.17	41.3–44.87	45–50.25
Note (repetition) rate acceleration (%)	−1	−36 to −11	−15 to 33	−19 to 2

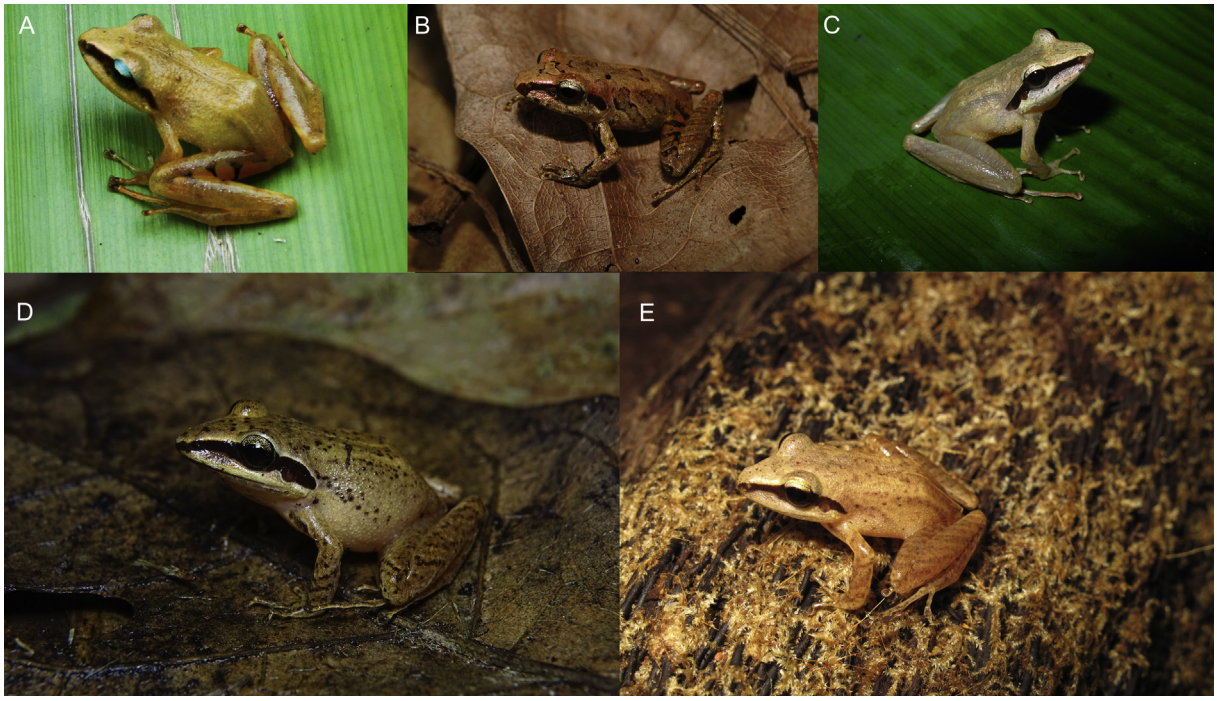

Fig. 7. Live specimens of the *Ischnocnema venancioi* series showing the mask-like pattern and the vivid yellow on the posterior surface of the thigh of *I. venancioi*. (A) *I. venancioi* (photo by L. O. Drummond), (B) *I. venancioi* (photo by L. O. Drummond), (C) *I. hoehnei* (photo by L. R. Malagoli), (D) *I. parnaso* sp. nov. (photo by L. O. Drummond), and (E) *I. colibri* sp. nov. (photo by C. F. B. Haddad).

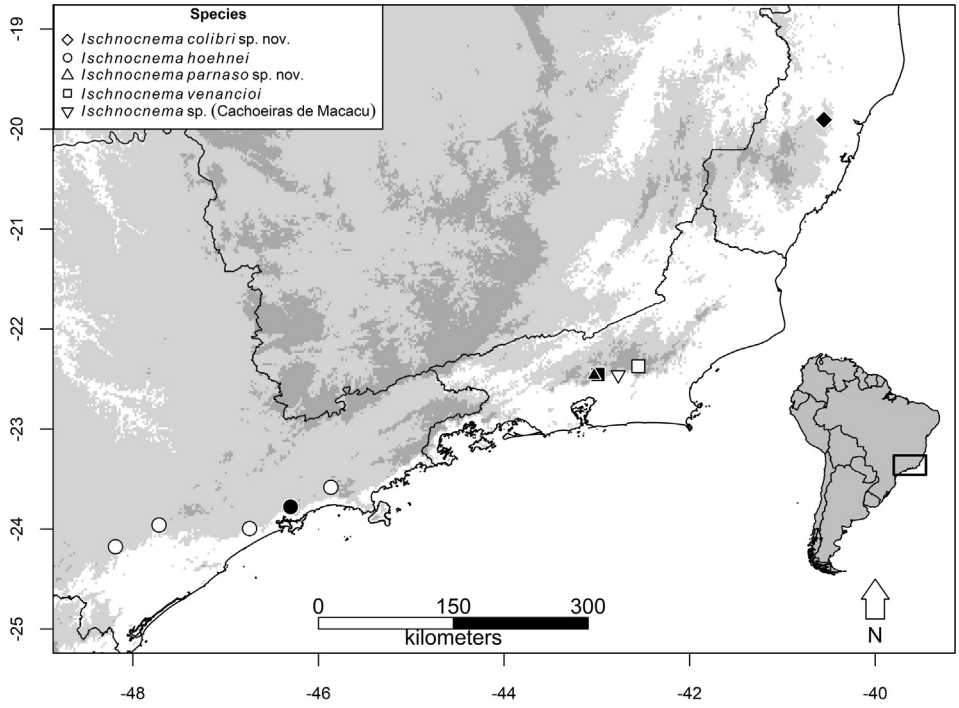

Fig. 8. Geographic distribution of the members of the *Ischnocnema venancioi* series. Solid symbols represent the type locality of each species. Area above 500 and 1000 m shaded gray.

morphological features distinguishing them from all other *Ischnocnema* species series. For these reasons we decided to create the *I. venancioi* series.

3.4.2.1. ***Ischnocnema venancioi*** *(B. Lutz, 1958)*. Redescription (Figs. 3B, 4A, 5A, B, 7A, B, and 9)

Eleutherodactylus venancioi B. Lutz, 1958

Eleutherodatylus (Eleutherodactylus) venancioi – Lynch and Duellman, 1997

Ischnocnema venancioi – Heinicke, Duellman, and Hedges, 2007

Lectotype: MNRJ 53573, adult male, designated herein, Serra dos Órgãos National Park (PARNASO), municipality of Teresópolis, state of Rio de Janeiro, Brazil, collected by Bertha Lutz in February 1956.

Paralectotypes: MNRJ 35185–35187, adult males collected in the

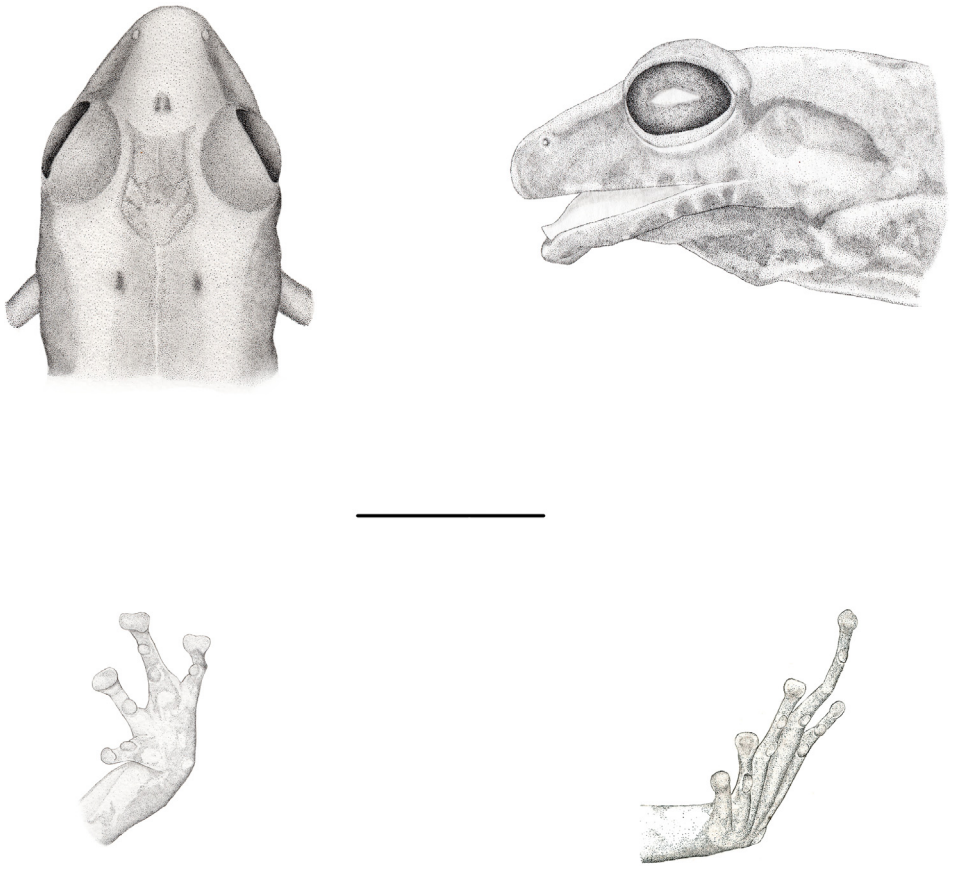

Fig. 9. Clockwise, from the upper left corner: dorsal and lateral views of the head and ventral views of the left hand and left foot of the lectotype of *Ischnocnema venancioi*, MNRJ 53573. Scale bar = 5 mm.

municipality of Teresópolis, state of Rio de Janeiro, Brazil, by B. Lutz and J. Venancio in November 1944. MNRJ 53565–53566, poorly preserved, sex undetermined, collected in the municipality of Teresópolis, state of Rio de Janeiro, Brazil, by B. Lutz on 21 October 1952. MNRJ 53572, 53574–53580, 53582–53589, adult males and MNRJ 53581, poorly preserved, sex undetermined, collected with the lectotype. MNRJ 53597, adult male, and MNRJ 53598, juvenile, collected in the municipality of Teresópolis, state of Rio de Janeiro, Brazil, by B. Lutz and J. Venancio in July 1943. MNRJ 53599–53600, poorly preserved, sex undetermined, collected at PARNASO, municipality of Teresópolis, state of Rio de Janeiro, Brazil, by B. Lutz and J. Venancio on 20 October 1946. MNRJ 56191–53194, adult males collected at PARNASO, municipality of Teresópolis, state of Rio de Janeiro, Brazil, by B. Lutz on 23–26 November 1956. MNRJ 56213, adult male, and MNRJ 56214, juvenile, collected at PARNASO, municipality of Teresópolis, state of Rio de Janeiro, Brazil, by B. Lutz and J. Venancio on 1–10 December 1944.

Diagnosis: In the *I. venancioi* series by phylogenetic placement (Fig. 1) and the following combination of characters: (1) Finger I smaller than Finger II; (2) tips of fingers expanded, discs of fingers III and IV large and truncated (Fig. 3B); (3) one large, conspicuous, glandular-appearing nuptial pad on Finger I; (4) black mask-like stripe starting at the tip of the snout or the nostril, contouring the *canthus rostralis*, passing through the eye (better seen in life, color fades in preservative, Fig. 7), contouring the dorsal portion of the tympanum, and finishing near arm insertion; (5) dorsum smooth or finely tuberculate.

Ischnocnema venancioi is distinguished from all other species of the *I. venancioi* series by the following combination of characters: (1) small size (SVL in males 15.7–22.3 mm, n = 31; female 24.1 mm, n = 1); (2) in preservative, posterior face of the thigh with cream oval spots on a dark-brown background or with slim dark-brown bars on a cream background (Fig. 5A, B; cream spots and background yellow to orange in life); (3) Finger I much smaller than Finger II (Finger I half to two thirds the size of Finger II, not reaching the base of its disk); (4) foot small (foot length/SVL 0.40–0.54); (5) tibia small; (tibia length/SVL = 0.48–0.60); (6) fourth toe disk small (fourth toe disk width/third finger disk width = 0.53–0.93).

Description of lectotype: Small size (SVL 17.4 mm). Head longer than wide; head length 46% of SVL, head width 37% of SVL; snout subelliptical in dorsal view, acuminate in lateral view; nostril rounded, oriented laterally, located near the tip of the snout; *canthus rostralis* slightly distinct, straight; loreal region slightly concave; postrictal tubercles absent; eye protuberant, oriented laterally; eye diameter 31% of head length; palpebral tubercles absent; tympanum distinct, rounded; tympanic membrane undifferentiated; annulus present, visible externally; tympanum diameter 34% of eye diameter; supratympanic fold absent; vocal slits present; vocal sac not apparent; tongue elliptical, without posterior notch; choanae rounded; dentigerous processes of the vomer located posteromedially to choanae, triangle-shaped, medially separated by a gap approximately the width of one dentigerous process; vomerine teeth present.

Forelimb slender; palmar tubercle indistinct; thenar tubercle indistinct; single glandular-appearing nuptial pad, extending dorsally from the distal to the proximal portion of metacarpus on Finger I; palm smooth; supernumerary tubercles absent; single subarticular tubercles prominent, rounded, large; fingers slender, without fringes; tip of Finger I slightly expanded; tips of fingers II– IV fairly expanded, truncated, with a V-shaped median slit in dorsal view; fourth toe disk small, width 56% of third finger disk; Finger I approximately two thirds the size of Finger II; finger lengths I < II < IV < III.

Hindlimb slender; shank longer than thigh; tibia length 57% of SVL,

thigh length 51% of SVL; calcar tubercle absent; tarsal folds absent; foot small, length 45% of SVL; inner metatarsal tubercle elliptical, much larger than rounded outer metatarsal tubercle; sole of foot smooth; supernumerary tubercles absent; single subarticular tubercles present, large, prominent, rounded; toes long, slender, without fringes; tip of Toe I slightly expanded; tips of toes II–V fairly expanded, truncated, with a V-shaped median slit in dorsal view; toe lengths I < II < V < III < IV.

Dorsal skin smooth, with a few sparse tubercles; vertebral line from behind the eyes to vent; venter smooth; discoidal and thoracic folds absent.

Coloration of lectotype in preservative: The specimen is rather faded so the dorsal pattern is unclear. Dorsum yellowish-brown; one large brown heart-shaped spot starting just posterior to eyes and reaching level of the top of tympanum; two brown dots at the level of arm insertion; one brown transverse narrow band at the level of the sacral vertebra; head yellowish-brown, with one brown spot on the dorsal surface just anterior to eyes; loreal region with brown mask-like stripe from the tip of the nose to near the arm insertion; forelimb yellowish-brown; hindlimb yellowish-brown; posterior surface of the thigh with cream-colored oval spots surrounded by a brown background; venter and gular region cream-colored, with sparse brown dots.

Measurements of lectotype (in millimeters): SVL 17.4, head length 8.0, head width 6.5, eye diameter 2.5, tympanum diameter 0.9, eye-nostril distance 1.5, internarial distance 1.8, eye-to-eye distance 2.8, forearm length 3.8, hand length 4.2, third finger disk length 0.9, thigh length 8.8, tibia length 10.0, tarsal length 5.9, foot length 7.9, and fourth toe disk length 0.5.

Variation: Additional referred specimens are listed in Appendix B. Nostril opening can also be elliptical, as can also be the tympanum. Tongue is elliptical, ovoid, or rounded. Finger I is half to two-thirds as large as Finger II. Some specimens have palpebral tubercles. Palmar and thenar tubercles are sometimes slightly distinct, the former heart-shaped and the latter elliptical, both the same size. Posterior surface of the thigh in preservative with cream-colored spots over a brown background or brown bars over a cream-colored background (Fig. 5A, B; cream-colored portions yellow to orange in life, Fig. 7A, B). Dorsum can also be finely tuberculate. Lutz (1958) stated, and we confirm, that *I. venancioi* has three dorsal patterns: one with "longitudinal bands of diverse tones" (Fig. 4A; Figs. 1, 3, and 6 in Lutz (1958)); the "tapestry-like" pattern, with "intrincate figures, centered around the narrow light vertebral line" (Fig. 7B; Figs. 2, 4, and 5 in Lutz (1958)); and no distinct pattern (Fig. 7A). Sometimes the nuptial pad is difficult to see because it is exactly the same color as the skin. Female specimen (SVL 24.1 mm, n = 1) is much larger than male specimens (SVL 15.7–22.3 mm, n = 31). Variation in SVL and body proportions is given in Table 4. In life the iris is bicolored, with a lighter superior half with shades going from metallic blue to light brown, and a darker lower half usually of a dark brown shade similar to that of the canthal stripe.

Advertisement call: Not formally described. In the original description (Lutz, 1958) the sound is described as a "*crrr crrr*", which makes sense when you listen to the calls of the other species in the *I. venancioi* series (described below).

Comparison with other species: Finger I smaller than Finger II distinguishes *I. venancioi* from members of the *I. guentheri*, *I. parva*, and *I verrucosa* series and from *I. manezinho* (Finger I approximately the same size as Finger II in these species; Garcia, 1996; Hedges et al., 2008). Expanded tips of fingers II–IV and large truncated discs of fingers III and IV distinguish *I. venancioi* from members of the *I. parva* series, *I. nanahallux* (tips of fingers not expanded in these species; Hedges et al., 2008; Brusquetti et al., 2013), and members of the *I. verrucosa* series (disks small or moderately-sized in these species; Hedges et al., 2008; Canedo et al., 2012). The large, conspicuous, glandular-appearing nuptial pad differentiates *I. venancioi* from *I. manezinho*, *I. sambaqui*, *I. nanahallux*, and the members of the *I. lactea* series (minute nuptial pad in *I. randorum*; translucent in *I.* nigriventris and *I. vizottoi*; reduced to some white granules in *I. holti*; absent in *I.* manezinho, *I. sambaqui*, *I. nanahallux*, *I. melanopygia* and *I. spanios*; unknown in other species; Heyer, 1985; Hedges et al., 2008; Targino and Carvalho-e-Silva, 2008; Berneck et al., 2013) and *I. verrucosa* series (except for *I. surda*; faint, translucent nuptial pad in *I. karst* [Canedo, Targino, Leite, and Haddad, 2012]; absent in other species; Hedges et al., 2008; Canedo et al., 2010, 2012). The mask-like stripe starting at the tip of the snout or the nostril, contouring the *canthus rostralis*, passing through the eye, contouring the dorsal portion of the tympanum, and finishing near arm insertion distinguishes *I. venancioi* from *I. manezinho*, *I. sambaqui*, and the members of the *I. guentheri*, *I. lactea*, and *I. verrucosa* series (mask-like stripe usually absent in these species; when present it does not pass through the eye). The smooth or finely tuberculate dorsum distinguishes *I. venancioi* from *I. sambaqui* (rugose in *I. sambaqui*; Castanho and Haddad, 2000) and from the members of the *I. verrocusa* series (tuberculate in these species; Hedges et al., 2008; Canedo et al., 2010, 2012).

Ischnocnema venancioi (SVL of males 15.7–22.3 mm, female 24.1 mm) differs from all other species of the *I. venancioi* series by its smaller size (SVL of males of other species of the *I. venancioi* species series 22.9–34.8 mm; of females 31.1–42.7 mm), by the posterior surface of the thigh with cream-colored ovoid spots on a dark-brown background or with dark-brown slim bar on a cream-colored background in preservative (cream-colored spots and background yellow to orange in life; posterior surface of the thigh mottled in other species of the *I. venancioi* species series), and by Finger I being much smaller than Finger II (Finger I reaching approximately the base of the disk of Finger II in other species of the *I. venancioi* species series).

By its smaller foot, *I. venancioi* (foot length/SVL = 0.40–0.54) differs from *I. hoehnei* (foot length/SVL = 0.67–0.70) and from *I. parnaso* sp. nov. (foot length/SVL = 0.55–0.63). By its smaller tibia, *I. venancioi* (tibia/SVL = 0.48–0.60) differs from *I. hoehnei* (tibia/SVL = 0.67–0.73) and by the smaller fourth toe disk, *I. venancioi* (fourth toe disk length/third finger disk length = 0.53–0.93) differs from *I. parnaso* sp. nov. (fourth toe disk length/third finger disk length = 1.00–1.09).

Geographic distribution: *Ischnocnema venancioi* is currently known from the highlands above 800 m of the Serra dos Órgãos mountain range in the state of Rio de Janeiro, in the municipalities of Teresópolis and Nova Friburgo.

Natural history notes: The species is usually found in association with bromeliad plants (Lutz, 1958; this study). Individuals start calling at dusk while perched on the leaves of ground bromeliads or other low vegetation (Lutz, 1958).

Remarks: In the original description of *Eleutherodactylus venancioi* (=*Ischnocnema venancioi*), Lutz (1958) included in the "Type locality and types" section (*Localidade tipo e tipos* section in the part in Portuguese) "6 female cotypes, 60 paratypes, males or not sexed" but did not designate a holotype or give museum numbers. Based on the article 72.1.1 of the International Code of Zoological Nomenclature, we consider all 66 specimens as the type series, because the author referred to all of them as types (Lutz 1958). Additionally, separating the specimens in "cotypes" and "paratypes" is not a situation provided by article 72.4.6, so we consider all 66 specimens as syntypes. We found 33 specimens at the Museu Nacional, Rio de Janeiro, Brazil, collected before 1958 (the year of the species description), and since Bertha Lutz worked at the Museu Nacional, and all the specimens were collected by her, we assume that these were part of the specimens that she used to describe *E. venancioi*. Most specimens are well-preserved and bear all the diagnostic characters that we used to identify the species. So, among these well-preserved specimens, we hereby designate the MNRJ 53573 as the lectotype of *E. venancioi*. All other specimens (partially listed above) are paralectotypes.

Frost (2018) mentions that the species is known from the coastal mountains of Rio de Janeiro and São Paulo, Brazil, but we are not aware of *I. venancioi* occurring in any locality outside the state of Rio de Janeiro.

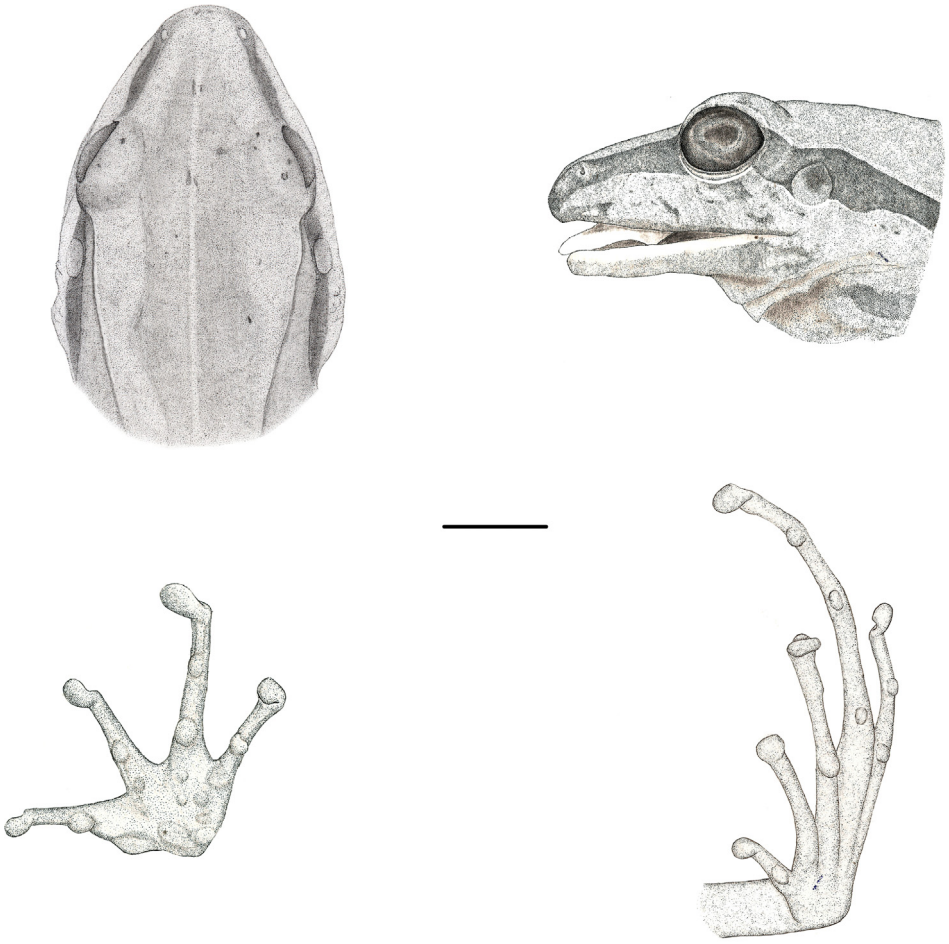

Fig. 10. Clockwise, from the upper left corner: dorsal and lateral views of the head and ventral views of the left hand and left foot of the holotype of *Ischnocnema hoehnei*, AL-MN 2525. Scale bar = 5 mm.

3.4.2.2. ***Ischnocnema hoehnei*** *(Lutz, 1958)*. Redescription (Figs. 3A, 4D, 5C, 7C, and 10)

Eleutherodactylus hoehnei Lutz, 1958

Eleutherodatylus (Eleutherodactylus) hoehnei – Lynch and Duellman, 1997

Ischnocnema hoehnei – Heinicke, Duellman, and Hedges, 2007

Holotype: AL-MN 2525, adult female collected at Reserva Biológica do Alto da Serra de Paranapiacaba (RBASP, formerly Estação Biológica do Alto da Serra), Paranapiacaba, municipality of Santo André, state of São Paulo, Brazil, by F. C. Hoehne in April 1934.

Paratypes: AL-MN 2526 (collected with the holotype; not examined), AL-MN 3376 (cleared for osteological studies according to the original publication; not examined), MZUSP 10201–10206, 10177–10178, 11000, 11064 (not examined).

Diagnosis: In the *I. venancioi* series by phylogenetic placement (Fig. 1) and the following combination of characters: (1) Finger I smaller than Finger II; (2) tips of fingers expanded, discs of fingers III and IV large and truncated (Fig. 3A); (3) one large, conspicuous, glandular-appearing nuptial pad on Finger I; (4) black mask-like stripe starting at the tip of the snout or the nostril, contouring the *canthus rostralis*, passing through the eye (better seen in life, Fig. 7), contouring the dorsal portion of the tympanum, and finishing near arm insertion; (5) dorsum smooth or finely tuberculate. *Ischnocnema hoehnei* is distinguished from all other species of the *I. venancioi* series by the following combination of characters: (1) large size (SVL of males 30.6–34.8 mm, n = 3; female 42.7 mm, n = 1); (2) foot large (foot length/SVL 0.67–0.70); (3) tibia large (tibia length/SVL = 0.67–0.73); (4) posterior face of thigh mottled, forming small irregular spots in some specimens (Fig. 5C); (5) Finger I slightly smaller than Finger II (tip of Finger I reaching the base of the disk of Finger II approximately); (6) fourth toe disk small (fourth toe disk width/third finger disk width = 0.93–0.96); (7) low advertisement call frequency (1.90 kHz); (8) advertisement call with a high number of notes (59); (9) medium note (repetition) rate (35.85 notes per second).

Redescription of holotype: large size (42.7 mm), head longer than wide; head length 43% of SVL; head width 36% of SVL; snout subelliptical in dorsal view, acuminate in lateral view; nostril elliptical, oriented laterally, located near tip of snout; *canthus rostralis* distinct, straight; loreal region slightly concave; postrictal tubercles absent; eye protuberant, oriented laterally; eye diameter 34% of head length; one palpebral tubercle; tympanum distinct, rounded; tympanic membrane undifferentiated; annulus present, visible externally; tympanum diameter 38% of eye diameter; supratympanic fold absent; tongue large, ovoid, without posterior notch; choanae rounded; dentigerous processes of the vomer located posteriormedially to choanae, triangle-shaped, medially separated by a gap approximately the width of one dentigerous process; vomerine teeth present.

Forelimb slender; palmar tubercle slightly distinct, heart-shaped; thenar tubercle elliptical, less than half the size of palmar tubercle; palm smooth; three slightly distinct supernumerary tubercles; single subarticular tubercles prominent, rounded, large; fingers slender, without fringes; tip of Finger I slightly expanded; tips of fingers II–IV fairly expanded, truncated, with a V-shaped median slit in dorsal view; fourth toe disk small; fourth toe disk width 93% of third finger disk; Finger I slightly smaller than Finger II, its length reaching the base of Finger II disk; finger lengths I < II < IV < III.

Hindlimb slender; shank longer than thigh; tibia length 73% of SVL; thigh length 59% of SVL; posteroventral surface of the thighs areolate; calcar tubercle small; tarsal folds absent; foot large; foot length 67% of SVL; inner metatarsal tubercle elliptical, much larger than outer metatarsal tubercle, rounded; sole of foot smooth; a few small supernumerary tubercles; single subarticular tubercles present, large, prominent, rounded; toes long, slender, with discrete fringes; tip of Toe I slightly expanded; tips of toes II–V fairly expanded, truncated, with a V-shaped median slit in dorsal view; toe lengths I < II < V < III < IV.

Dorsal skin smooth, with a few sparse tubercles; vertebral line from just anterior to eyes extending almost to vent; venter finely tuberculate; discoidal and thoracic folds present.

Coloration of holotype in preservative: The specimen is somewhat faded. Dorsum with shades of beige and brown, with a broad brown band of irregular width starting posterior to the eyes and finishing at the vent, narrowing three times throughout its length, and irregularly spaced brown dots; loreal region with brown mask-like stripe from the tip of the nose to near arm insertion; forelimb beige; hindlimb striped beige and faded brown dorsally; cream-colored ventrally; posterior surface of the thighs beige; venter beige.

Measurements of holotype (in millimeters): SVL 42.7, head length 18.5, head width 15.2, eye diameter 6.3, tympanum diameter 2.4, eye-nostril distance 3.6, internarial distance 5.2, eye-to-eye distance 7.3, forearm length 9.5, hand length 13.2, third finger disk length 2.4, thigh length 25.1, tibia length 31.0, tarsal length 14.6, foot length 28.8, and fourth toe disk length 2.2.

Variation: Additional referred specimens are listed in Appendix B. Dorsum can be finely tuberculate, mask-like stripe can reach beyond the insertion of the arms, and tongue is elliptical in some specimens. Fingers of other specimens bear discrete fringes and the dorsal pattern is variable (see Lutz, 1958 for illustrations). Vocal sac in males is single, subgular, and slightly expanded externally, vocal slits present and nuptial pad single, apparently-glandular, same color as the hand. Female specimen (SVL 42.7 mm, n = 1) is much larger than male specimens (SVL 30.6–34.8 mm, n = 3). Variation in SVL and body proportions is given in Table 4.

Advertisement call: Only one advertisement call was available for our analysis. The call consists of several short notes emitted in regular intervals. The call begins with low energy notes, which increase in energy over time, until reaching a peak almost at the end of the call. The last note has notably less energy than the penultimate note (Fig. 6A). Call duration 1.65 s, call rise time 96%, dominant frequency 1.90 kHz, 59 notes per call, note (repetition) rate 35.85 notes per second, and note (repetition) rate acceleration −20%.

Comparison with other species: Finger I smaller than Finger II distinguishes *I. hoehnei* from members of the *I. guentheri*, *I. parva*, and *I verrucosa* series and from *I. manezinho* (Finger I approximately the same size as Finger II in these species; Garcia, 1996; Hedges et al., 2008). Expanded tips of fingers II–IV and large truncated discs of fingers III and IV distinguish *I. hoehnei* from members of the *I. parva* series, *I. nanahallux* (tips of fingers not expanded in these species; Hedges et al., 2008; Brusquetti et al., 2013), and members of the *I. verrucosa* series (disks small or moderately-sized in these species; Hedges et al., 2008; Canedo et al., 2012). The large, conspicuous, glandular-appearing nuptial pad differentiates *I. hoehnei* from *I. manezinho*, *I. sambaqui*, *I. nanahallux*, and the members of the *I. lactea* (minute nuptial pad in *I. randorum;* translucent in *I.* nigriventris and *I. vizottoi*; reduced to some white granules in *I. holti*; absent in *I. melanopygia* and *I. spanios*; unknown in other species; Heyer, 1985; Hedges et al., 2008; Targino and Carvalho-e-Silva, 2008; Berneck et al., 2013) and *I. verrucosa* series (except for *I. surda*; faint, translucent nuptial pad in *I. karst*; absent in other species; Hedges et al., 2008; Canedo et al., 2010, 2012). The mask-like stripe starting at the tip of the snout or the nostril, contouring the *canthus rostralis*, passing through the eye, contouring the dorsal portion of the tympanum, and finishing near arm insertion distinguishes *I. hoehnei* from *I. manezinho*, *I. sambaqui*, and the members of the *I. guentheri*, *I. lactea*, and *I. verrucosa* series (mask-like stripe usually absent in these species; when present it does not pass through the eye). The smooth or finely tuberculate dorsum distinguishes *I. hoehnei* from *I. sambaqui* (rugose; Castanho and Haddad, 2000) and from the members of the *I. verrocusa* series (tuberculate in these species; Hedges et al., 2008; Canedo et al., 2010, 2012).

By its large size (SVL of males 30.6–34.8 mm, n = 3; female 42.7 mm, n = 1), large foot (foot length/SVL 0.67–0.70), and large shank (tibia length/SVL 0.67–0.73), *I. hoehnei* differs from all other species of the *I. venancioi* species series (combined SVL of males 15.7–30.3 mm, n = 41; females 24.1–38.0 mm, n = 5).

The mottled posterior surface of the thigh, forming small irregular cream-colored spots in some specimens, of *I. hoehnei* distinguishes it from *I. venancioi* (posterior surface of the thigh with cream-colored oval spots surrounded by a dark-brown background or with dark-brown slim bars on a clear background; cream-colored spots and background yellow to orange in life), *I. parnaso* sp. nov. (posterior surface of the thigh with cream-colored large irregular-shaped spots surrounded by a mottled background), and *I. colibri* sp. nov. (posterior surface of the thigh mottled, interleaved with cream-colored bars, forming a striped pattern, or with large irregular-shaped cream-colored spots surrounded by a mottled background). Having Finger I slightly smaller than the Finger II, reaching approximately the base of Finger II, distinguishes *I. hoehnei* from *I. venancioi* (Finger I much smaller than Finger II, not reaching the base of Finger II) and by having the fourth toe disk small (fourth toe disk width/third finger disk width = 0.93–0.96) differentiates *I. hoehnei* from *I. parnaso* sp. nov. (fourth toe disk width/third finger disk width = 1.00–1.09).

Ischnocnema hoehnei differs from *I. parnaso* sp. nov. and *I. colibri* sp. nov. by the lower frequency of its advertisement call (1.90 kHz in *I. hoehnei*; 2.34–2.84 kHz in the two new species), by the higher number of notes per call (59 in *I. hoehnei*; 18–53 in the two new species), and by the intermediate note (repetition) rate (35.85 notes per second in *I. hoehnei*; 41.30–44.82 notes per second in *I. colibri* sp. nov. and 16.55–21.17 notes per second in *I. parnaso* sp. nov.).

Natural history notes: The natural history and habits of *I. hoehnei* are poorly known. Specimens are usually found perched on ground bromeliads or other ground plants (Heyer et al., 1990; Malagoli, L. R. personal communication). The species is commonly found in open areas inside forests, such as clearings or stream margins (Lutz, 1958; Heyer et al., 1990; Oliveira et al., 2008).

Geographic distribution: *Ischnocnema hoehnei* is currently known from the highlands (above 800 m of elevation) of Serra do Mar mountain range in the state of São Paulo, Brazil, from the municipalities of Santo André, Itanhaém, Salesópolis, Pilar do Sul, and São Miguel Arcanjo.

Remarks: Heyer et al. (1990) mentioned one male (SVL = 22.0 mm) and one female (SVL = 29.4 mm) specimen from Boracéia, municipality of Salesópolis. They stated that the male specimen lacked vocal slits and nuptial pads. All male specimens that we analyzed had both these characters, and our smallest specimen had an SVL of 30.6 mm, much larger than the male from Boracéia. The authors mentioned some diagnostic characters of *I. hoehnei*, like the mask-like stripe, the large foot, and the large shank. We did not examine these specimens, but we believe that they are indeed *I. hoehnei* and that the male specimen lacked vocal slits and nuptial pads because it was a subadult. Hedges et al. (2008) also mentioned that *I. hoehnei* lacks nuptial pads, probably following Heyer et al. (1990).

As noted by Lutz (1958) in the original description, the large size and the color pattern (including the mask-like stripe) of *I. hoehnei* is superficially similar to that of *Haddadus binotatus* (Spix, 1824). However, the two species have notable differences. *Haddadus binotatus* has a series of longitudinal glandular ridges in the dorsum, and Finger I is much larger than Finger II (dorsum lacking glandular ridges and Finger I slightly smaller than Finger II in *I. hoehnei*). Males of *H. binotatus* lack nuptial pads on Finger I (nuptial pads present in males of *I. hoehnei*).

Fig. 11. Clockwise, from the upper left corner: dorsal and lateral views of the head and ventral views of the left hand and left foot of the lectotype of *Ischnocnema parnaso* sp. nov., CFBH 40812. Scale bar = 5 mm.

3.4.2.3. ***Ischnocnema parnaso*** *sp. nov.* (Fig. 4C, 5D, 7D, and 11)

Holotype: CFBH 41812, adult male collected at Pedra do Sino, Serra dos Órgãos National Park (PARNASO), municipality of Guapimirim, state of Rio de Janeiro, Brazil (22°27′42″S, 43°01′50″W, 2180 m of elevation), by Drummond, L. O. and Nogueira-Costa, P. on 20 December 2015.

Paratypes: CFBH 41813, adult male, MNRJ 91759, adult female, both collected with the holotype. MNRJ 91756–91758, adult males collected at Pedra da Baleia, PARNASO, municipality of Guapimirim, state of Rio de Janeiro, Brazil (22°27′40″S, 43°01′38″W, 2142 m of elevation), by Drummond, L. O. and Nogueira-Costa, P. on 21 December 2015.

Diagnosis: In the *I. venancioi* series by phylogenetic placement (Fig. 1) and the following combination of characters: (1) Finger I smaller than Finger II; (2) tips of fingers expanded, discs of fingers III and IV large and truncated; (3) one large, conspicuous, glandular-appearing nuptial pad on Finger I; (4) black mask-like stripe starting at the tip of the snout or the nostril, contouring the *canthus rostralis*, passing through the eye, contouring the dorsal portion of the tympanum, and finishing near arm insertion; (5) dorsum smooth. *Ischnocnema parnaso* sp. nov. is distinguished from all other species of the *I. venancioi* series by the following combination of characters: (1) medium-size (SVL of males 27.1–30.3 mm, n = 5; female 38.0 mm, n = 1); (2) medium-size foot (foot length/SVL 0.55–0.63); (3) small tibia (tibia length/SVL = 0.55–0.59); (4) posterior surface of the thigh with large irregular-shaped cream-colored spots surrounded by a mottled background; (5) Finger I slightly smaller than Finger II (tip of Finger I reaching the base of Finger II approximately); (6) fourth toe disk large (fourth toe disk width/third finger disk width = 1.00–1.09); (7) high advertisement call frequency (2.34–2.67 kHz); (8) advertisement call with low number of notes (18–29); (9) low note (repetition) rate (16.55–21.17 notes per second).

Description of holotype: Medium-size (SVL = 29.1 mm). Head longer than wide; head length 39% of the SVL, head width 35% of the SVL; snout sub-elliptical in dorsal view, acuminate in lateral view; nostril rounded, oriented laterally, located near the tip of snout; *canthus rostralis* slightly distinct, straight; loreal region slightly concave; postrictal tubercles absent; eye protuberant, oriented laterally; eye diameter 31% of head length; palpebral tubercles absent; tympanum distinct, rounded; tympanic membrane undifferentiated; annulus present, visible externally; tympanum diameter 43% of eye diameter; supratympanic fold absent; vocal slits present; vocal sac slightly distinct, one visible fold parallel to left side of the jaw; tongue large, elliptical, without posterior notch; choanae rounded; dentigerous processes of the vomer located posteromedially to choanae, triangle-shaped, medially separated by a gap approximately the same size as one dentigerous process; vomerine teeth present.

Forelimb slender; palmar tubercle barely distinct, heart-shaped, its diameter approximately equal to that of the thenar tubercle; thenar tubercle barely distinct, elliptical; single glandular-appearing nuptial

pad, extending dorsally from the distal to the proximal portion of metacarpus on Finger I, the same color as the surrounding skin; palm smooth; supernumerary tubercles absent; single subarticular tubercles prominent, rounded, large; fingers slender, without fringes; tip of Finger I not expanded; tip of Finger II slightly expanded; tips of fingers III and IV fairly expanded, truncated, with a V-shaped median slit in dorsal view; Finger I slightly smaller than Finger II, its length reaching the base of Finger II disk; finger lengths I < II < IV < III.

Hindlimb slender; shank longer than thigh; tibia length 58% of SVL; thigh length 55% of SVL; calcar tubercle absent; tarsal folds absent; foot medium-size; foot length 60% of SVL; inner metatarsal tubercle elliptical, twice as big as outer metatarsal tubercle; outer metatarsal tubercle rounded; sole of foot smooth; supernumerary tubercles absent; single subarticular tubercles present, large, prominent, rounded; toes long, slender, without fringes; tip of Toe I slightly expanded; tips of toes II–V fairly expanded, truncated, with a V-shaped median slit in dorsal view; toe lengths I < II < V < III < IV.

Dorsal skin smooth; vertebral line absent; venter smooth; discoidal and thoracic folds absent.

Coloration of holotype: Background cream-colored; dorsum with several sparse dark-brown dots; loreal region with dark-brown mask-like stripe from the tip of the snout to near the arm insertion; dark-brown dots forming a blotch on the dorsal part of the head, between the eyes; forelimb cream-colored, with several dark-brown dots larger than those of the dorsum over the dorsal surfaces of the arm, forearm, and hand; ventral surfaces of the arm, forearm, and hand with more sparse dark-brown dots; hindlimb cream-colored, with several dark-brown dots larger than those of the dorsum and smaller than those of the forelimb over dorsal and ventral surfaces of the thigh, tibia, and dorsal surface of the foot; dark-brown dots less sparse on the sole of the foot; posterior surface of the thigh with cream-colored irregular spots surrounded by dark-brown mottled background; venter cream-colored with a few dark-brown dots on the chest; gular region cream-colored; jaw bordered by concentrated small dark-brown dots forming a thin line.

Measurements of holotype (in millimeters): SVL 29.1, head length 11.3, head width 10.2, eye diameter 3.5, tympanum diameter 1.5, eye-nostril distance 2.5, internarial distance 2.8, eye-to-eye distance 5.0, forearm length 5.5, hand length 8.6, third finger disk length 1.4, thigh length 15.9, tibia length 17.0, tarsal length 8.0, foot length 17.6, and fourth toe disk length 1.5.

Variation: Tongue is rounded, elongated, or triangular, and choanae is elliptical in some specimens. Postrictal tubercle is present in female specimen. Thoracic fold is present in some specimens. Sometimes the nuptial pad is difficult to see because it is exactly the same color as the surrounding skin. Female specimen (SVL 38.0 mm, n = 1) is much larger than male specimens (SVL 27.1–30.3 mm, n = 5). Variation in SVL and body proportions is given in Table 4.

Etymology: The name "PARNASO" is the abbreviation for Parque Nacional da Serra dos Órgãos (Serra dos Órgãos National Park), type locality of the species. The park was created on November 30, 1939, and it is the third oldest park in Brazil, housing astonishing biodiversity. It is also the type locality of several anurans and one of the most important Atlantic Forest conservation units in Brazil. The name is used here as a noun in apposition.

Advertisement call: The advertisement call (19 calls of five males; Table 6; Fig. 6B) is emitted sporadically and is composed of 18–29 notes ($\overline{X}$ = 25.00 ± 3.04) emitted at regular intervals. The call begins with low-energy notes, which increase in energy over time, until reaching a peak almost at the end of the call. The last note usually has notably less energy than the penultimate note. The call rise time is 42–92% ($\overline{X}$ = 66.06 ± 15.34) and the dominant frequency 2.34–2.67 kHz ($\overline{X}$ = 2.46 ± 0.09). The advertisement call lasts 1.00 to 1.50 s ($\overline{X}$ = 1.25 ± 0.12), and the note (repetition) rate is 16.55–21.17 notes per second ($\overline{X}$ = 19.58 ± 1.32). The note rate decelerates at the end of the call, with a note-rate acceleration of −36 to −11% ($\overline{X}$ = −22.98 ± 5.99).

Comparison with other species: Finger I smaller than Finger II distinguishes *I. parnaso* sp. nov. from members of the *I. guentheri*, *I. parva*, and *I verrucosa* series and from *I. manezinho* (Finger I approximately the same size as Finger II in these species; Garcia, 1996; Hedges et al., 2008). Expanded tips of fingers II–IV and large truncated discs of fingers III and IV distinguish *I. parnaso* sp. nov. from members of the *I. parva* series, *I. nanahallux* (tips of fingers not expanded in these species; Hedges et al., 2008; Brusquetti et al., 2013), and members of the *I. verrucosa* series (disks small or moderately-sized in these species; Hedges et al., 2008; Canedo et al., 2012). The large, conspicuous, glandular-appearing nuptial pad differentiates *I. parnaso* sp. nov. from *I. manezinho*, *I. sambaqui*, *I. nanahallux*, and the members of the *I. lactea* (minute nuptial pad in *I. randorum;* translucent in *I.* nigriventris and *I. vizottoi*; reduced to some white granules in *I. holti*; absent in *I. melanopygia* and *I. spanios*; unknown in other species; Heyer, 1985; Hedges et al., 2008; Targino and Carvalho-e-Silva, 2008; Berneck et al., 2013) and *I. verrucosa* series (except for *I. surda*; faint, translucent nuptial pad in *I. karst*; absent in other species; Hedges et al., 2008; Canedo et al., 2010, 2012). The mask-like stripe starting at the tip of the snout or the nostril, contouring the *canthus rostralis*, passing through the eye, contouring the dorsal portion of the tympanum and reaching near arm insertion distinguishes *I. parnaso* sp. nov. from *I. manezinho*, *I. sambaqui*, and the members of the *I. guentheri*, *I. lactea*, and *I. verrucosa* series (mask-like stripe usually absent in these species; when present it does not pass through the eye). The smooth or finely tuberculate dorsum distinguishes *I. parnaso* sp. nov. from *I. sambaqui* (rugose; Castanho and Haddad, 2000) and from the members of the *I. verrocusa* series (tuberculate in these species; Hedges et al., 2008; Canedo et al., 2010, 2012).

Table 6
Acoustic parameters of the advertisement call of five recorded males of *Ischnocnema parnaso* sp. nov. Data are given as range (mean ± standard deviation) where appropriate.

Call recording	LOD 001	LOD 002	LOD 003	LOD 004	LOD 005
Number of analyzed calls	2	6	3	5	3
Call duration (s)	1.00–1.05	1.14–1.27 (1.20 ± 0.05)	1.17–1.25 (1.22 ± 0.05)	1.25–1.38 (1.33 ± 0.05)	1.25–1.50 (1.40 ± 0.13)
Call rise time (%)	42–62	44–79 (64 ± 15)	51–92 (75 ± 22)	57–85 (72 ± 10)	51–83 (62 ± 18)
Dominant frequency (kHz)	2.39	2.39–2.53 (2.48 ± 0.04)	2.44–2.67 (2.58 ± 0.09)	2.39–2.58 (2.45 ± 0.08)	2.34–2.44 (2.38 ± 0.05)
Notes per call	18.00	24.00–25.00 (24.33 ± 0.52)	23.00–25.00 (24.33 ± 1.15)	26.00–29.00 (28.00 ± 1.22)	26.00–27.00 (26.67 ± 0.58)
Note rate (notes/s)	16.55–17.58	19.06–20.43 (19.79 ± 0.53)	19.40–19.84 (19.60 ± 0.22)	20.59–20.88 (20.75 ± 0.14)	17.58–21.17 (18.89 ± 1.98)
Note repetition rate acceleration (%)	−26 to −20	−24 to −15 (-20 ± 4)	−18 to −11 (−16 ± 4)	−36 to −23 (−27 ± 5)	−33 to −24 (−28 ± 4)

Ischnocnema parnaso sp. nov. differs from all other species of the *I. venancioi* series by its large fourth toe disk (fourth toe disk width/third finger disk width = 1.00–1.09 in the new species; 0.53–0.96 in other species). Also, *I. parnaso* sp. nov. (SVL of males 27.1–30.3 mm, n = 5; female 38.0 mm) is smaller than *I. hoehnei* (SVL of males 30.6–34.8 mm, n = 3; female 42.7 mm, n = 1) and larger than *I. venancioi* (SVL of males 15.7–22.3 mm, n = 31; female 24.1 mm, n = 1) and *I. colibri* sp. nov. (SVL of males 22.9–25.2 mm, n = 5; SVL of females 31.1–34.6 mm, n = 3); and has a smaller foot (foot length/SVL 0.55–0.63) than *I. hoehnei* (foot length/SVL 0.67–0.70) and a larger foot than *I. venancioi* (foot length/SVL 0.40–0.54).

The posterior surface of the thigh with cream-colored large irregular-shaped spots surrounded by a mottled background distinguishes *I. parnaso* sp. nov. from *I. hoehnei* (posterior surface of the thigh mottled, forming small irregular cream-colored spots in some specimens) and *I. venancioi* (posterior surface of the thigh with cream-colored oval spots surrounded by a dark-brown background or with dark-brown slim bars on a clear background; spots and background yellow to orange in life). The small tibia (tibia length/SVL 0.55–0.59) differentiates *I. parnaso* sp. nov. from *I. hoehnei* (tibia length/SVL 0.67–0.73), and having Finger I slightly smaller than Finger II (Finger I tip reaching the base of the disk of the Finger II) differentiates the new species from *I. venancioi* (Finger I much smaller than Finger II; its size half to two thirds the size of Finger II).

Ischnocnema parnaso sp. nov. differs from *I. hoehnei* and *I. colibri* sp. nov. by the lower note (repetition) rate (16.55–21.17 notes per second in the new species; 35.78–44.82 notes per second in other species) and the lower number of notes per call (18–29 in the new species; 40–59 in other species). Additionally, the higher frequency of advertisement call (2.34–2.67 kHz) distinguishes *I. parnaso* sp. nov. from *I. hoehnei* (1.90 kHz).

Natural history notes: This species was found exclusively associated with high-elevation grasslands (*Campos de Altitude*), an open phytophysiognomy found on the granitic soils of the higher elevations of mountainous regions of Atlantic Forest. At the time of collection, we observed a high abundance of individuals calling at the type locality and its immediate surroundings. The species was active at dusk and night, and males were observed calling perched on low vegetation, mainly grasses (*e.g. Cortaderia modesta*). The female was observed on rocky soil.

Geographic distribution: The species is currently known only from the surroundings of Pedra do Sino (type locality) and Pedra da Baleia, in grasslands located above 2000 m of elevation at the PARNASO, in the municipality of Guapimirim, state of Rio de Janeiro, Brazil.

Remarks: The phylogenetic placement of *I. parnaso* sp. nov. within the *I. venancioi* series is uncertain. It is the sister group of all other members of the *I. venancioi* series in the Bayesian inference analysis (posterior probability of the whole clade 1.0 and of the immediately less inclusive clade 0.71) and the sister species of *I. hoehnei* in the maximum likelihood and the maximum parsimony analyses (40 and 58% bootstrap and jackknife, respectively). Future studies with more data are paramount for understanding the phylogenetic placement of *I.*

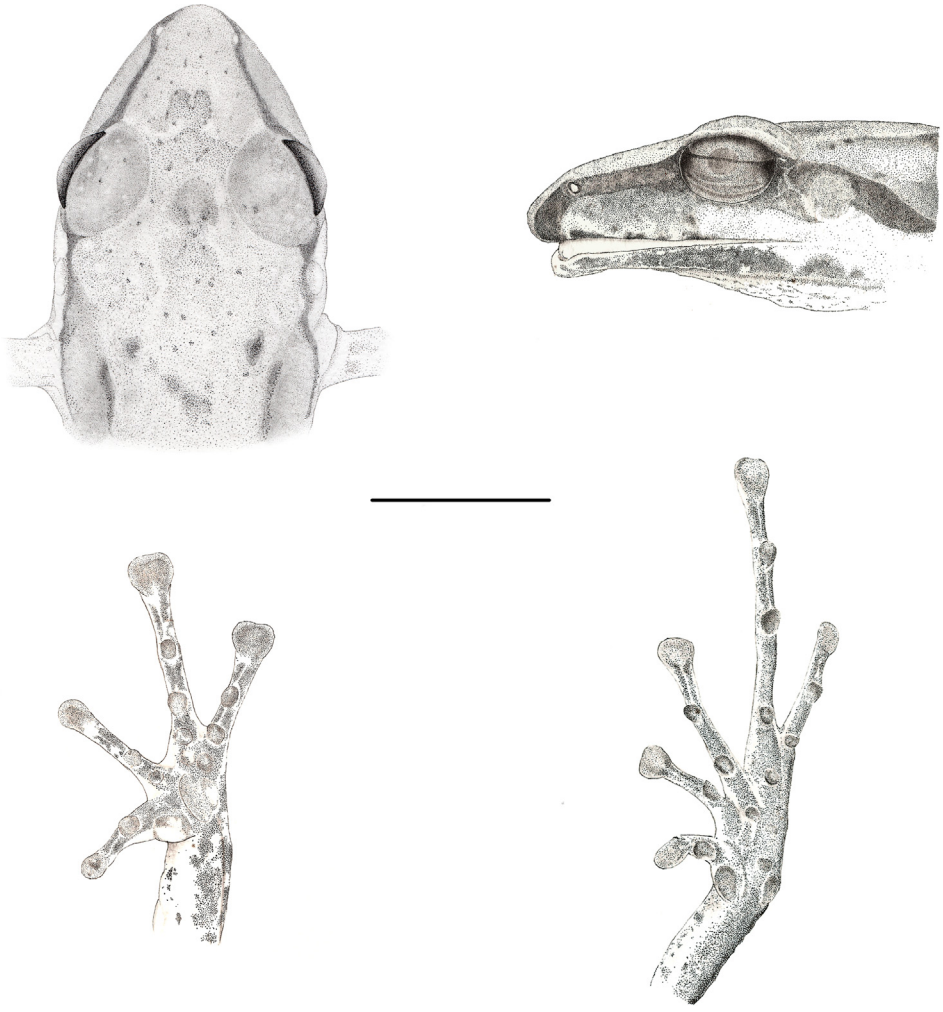

Fig. 12. Clockwise, from the upper left corner: dorsal and lateral views of the head and ventral views of the left hand and left foot of the lectotype of *Ischnocnema colibri* sp. nov., CFBH 40810. Scale bar = 5 mm.

parnaso sp. nov.

3.4.2.4. ***Ischnocnema colibri*** *sp. nov.* (Fig. 4B, 5E, 7E, and 12)

Holotype: CFBH 41810, adult male collected at Augusto Ruschi Biological Reserve, municipality of Santa Teresa, state of Espírito Santo, Brazil (19°54′25″S, 40°33′09″W, 803 m), by Taucce, P. P. G. and Parreiras, J. S. on 21 January 2017.

Paratypes: CFBH 41809, adult male collected at Augusto Ruschi Biological Reserve, municipality of Santa Teresa, state of Espírito Santo, Brazil (19°54′25″S, 40°33′09″W, 803 m), by Taucce, P. P. G. and Parreiras, J. S. on 20 January 2017. CFBH 41811, adult male, collected with holotype. MBML 10568–10569, adult males collected in the municipality of Santa Teresa, state of Espírito Santo, Brazil, by Ferreira, R. B., Ferreira, F. C. L. and Zandomenico, C. Z. on 12 December 2012. MBML 10570–10571, adult females collected in the municipality of Santa Teresa, state of Espírito Santo, Brazil, by Ferreira, R. B., Ferreira, F. C. L. and Zandomenico, C. Z. on 1 July 2013. MBML 10572, adult female collected near Augusto Ruschi Biological Reserve, municipality of Santa Teresa, state of Espírito Santo, Brazil, by Ferreira, R. B., Ferreira, F. C. L. and Zandomenico, C. Z. on 30 October 2015.

Diagnosis: In the *I. venancioi* series by phylogenetic placement (Fig. 1) and the following combination of characters: (1) Finger I smaller than Finger II; (2) tips of fingers expanded, discs of fingers III and IV large and truncated; (3) one large, conspicuous, glandular-appearing nuptial pad on Finger I; (4) dark-brown mask-like stripe starting at the tip of the snout or the nostril, contouring the *canthus rostralis*, passing through the eye, contouring the dorsal portion of the tympanum, and finishing near arm insertion; (5) dorsum smooth or finely tuberculate. *Ischnocnema colibri* sp. nov. is distinguished from all other species of the *I. venancioi* series by the following combination of characters: (1) medium-size (SVL of males 22.9–25.2 mm, n = 5; females 31.1–34.6 mm, n = 3); (2) foot medium-size (foot length/SVL 0.52–0.60); (3) tibia medium-size (tibia length/SVL = 0.56–0.62); (4) posterior surface of the thigh mottled, interleaved with cream-colored bars, forming a striped pattern, or with cream-colored large irregular-shaped spots surrounded by a mottled background; (5) Finger I slightly smaller than Finger II (tip of Finger I reaching the base of Finger II approximately); (6) small fourth toe disk (fourth toe disk width/third finger disk width = 0.73–0.96); (7) high advertisement call frequency (2.67–2.84 kHz); (8) advertisement call with medium number of notes (40–53); (9) high note (repetition) rate (41.30–44.82 notes per second).

Description of holotype: Medium-size (23.3 mm). Head longer than wide; head length 39% of SVL; head width 32% of SVL; snout subelliptical in dorsal view, acuminate in lateral view; nostril ovoid, oriented laterally, located near the tip of the snout; *canthus rostralis* slightly distinct, straight; loreal region slightly concave; eye protuberant, oriented laterally; eye diameter 32% of the head length; upper eyelid with a few diminutive tubercles; tympanum distinct, rounded; tympanic membrane undifferentiated; annulus present, visible externally; tympanum diameter 38% of eye diameter; supratympanic fold absent; vocal slits present; vocal sac slightly distinct, one visible fold parallel to each side of the jaw; tongue large, elliptical, without posterior notch; choanae elliptical; dentigerous processes of the vomer located posteromedially to choanae, triangle-shaped, medially separated by a gap approximately the width of one dentigerous process; vomerine teeth present, five on the right side and five on the left side.

Forelimb slender; palmar tubercle barely distinct, heart-shaped, its diameter approximately equal to that of thenar tubercle; thenar tubercle elliptical, distinct; glandular-appearing nuptial pad, extending dorsally from the distal to the proximal portion of metacarpus on Finger I, distinct; palm smooth; five supernumerary tubercles present; single subarticular tubercles prominent, rounded, large; fingers slender, without fringes; tip of Finger I not expanded; tip of Finger II slightly expanded; tips of fingers III and IV fairly expanded, truncated, with a V-shaped median slit in dorsal view; Finger I slightly smaller than Finger II, its length reaching the base of Finger II disk; finger lengths I < II < IV < III.

Hindlimb slender; shank longer than thigh; tibia length 56% of SVL; thigh length 52% of SVL; calcar tubercle absent; tarsal folds absent; foot medium-size; foot length 53% of SVL; inner metatarsal tubercle elliptical, twice as large as outer metatarsal tubercle, rounded; sole of foot smooth; four supernumerary tubercles present; single subarticular tubercles present, large, prominent, rounded; toes long, slender, without fringes; tip of Toe I slightly expanded; tips of toes II–V fairly expanded, truncated, with a V-shaped median slit in dorsal view; toe lengths I < II < VI < III < IV.

Dorsal skin finely tuberculate; vertebral line absent; venter smooth; discoidal and thoracic folds present.

Coloration of holotype: Background cream-colored; dorsum with several dark-brown dots, some of them forming blotches with no defined pattern, with an x-like mark starting near the pectoral girdle and ending on the sacral vertebrae; loreal region with dark-brown mask-like stripe from the tip of the snout to near the arm insertion; dark-brown dots forming a blotch on the dorsal part of the head between the eyes; forelimb cream-colored; several dark-brown dots forming irregular blotches on the dorsal surfaces of the arm, forearm, dorsal, and ventral surfaces of the hand; hindlimb cream-colored, with several dark-brown dots forming a striped pattern on its dorsal surface and on the posterior surface of the thigh; ventral surface of the thigh and shank with small sparse dark-brown dots; ventral surface of the tarsus and sole of the foot with plenty of small dark-brown dots; venter cream-colored, with very sparse small dark-brown dots; gular region cream-colored, with sparse dark-brown dots; jaw bordered by concentrated small dark-brown dots.

Measurements of holotype (in millimeters): SVL 23.3, head length 9.5,

Table 7
Acoustic parameters of five recorded males of *Ischnocnema colibri* sp. nov. Data are given as range (mean ± standard deviation) where appropriate. AC and TC are advertisement and territorial calls, respectively.

Call recording	PPGT 009	PPGT 010	PPGT 011	PPGT 012	PPGT 013		PPGT 014	
Type of call	AC	AC	AC	AC	AC	TC	AC	TC
Number of analyzed calls	1	2	1	4	1	13	1	6
Call duration (s)	1.09	1.03–1.15	1.19	1.14–1.20 (1.18 ± 0.03)	1.04	0.18–0.51 (0.28 ± 0.12)	0.90	0.17–0.20 (0.17 ± 0.01)
Call rise time (%)	89	74–84	56	53–60 (57 ± 3)	59	5–92 (54 ± 26)	65	67–91 (81 ± 9)
Dominant frequency (kHz)	2.67	2.76	2.80	2.76	2.84	2.71–2.93 (2.83 ± 0.07)	2.71	2.63–2.71 (2.68 ± 0.04)
Notes per call	49.00	46.00–52.00	53.00	47.00–52.00 (49.50 ± 2.08)	46.00	9.00–23.00 (13.31 ± 5.20)	40.00	8.00–10.00 (8.33 ± 0.82)
Note rate (notes/s)	44.87	44.75–45.22	44.61	41.30–44.60 (42.25 ± 1.58)	44.06	45–50 (47 ± 2)	44.35	47.06–50.25 (48.11 ± 1.19)
Note (repetition) rate acceleration (%)	−1	−13 to −1	11	−15 to 33 (8 ± 20)	5	−19 to −5 (−13 ± 5)	7	−8 to 2 (−1 ± 4)

head width 7.7, eye diameter 2.9, tympanum diameter 1.1, eye-nostril distance 2.5, internarial distance 2.2, eye-to-eye distance 4.5, forearm length 4.9, hand length 7.4, third finger disk length 1.2, thigh length 12.1, tibia length 13.5, tarsal length 6.6, foot length 12.3, and fourth toe disk length 1.1.

Variation: Tongue may also be rounded or lanceolate. Tip of Finger I can be slightly expanded. A thick vertebral line is present in one of the female specimens. Dorsal skin can also be smooth. There are two kinds of dorsal patterns: one with an x-like mark on the back (like the holotype, Fig. 4B) and one with several small dark-brown dots, often forming rounded blotches, on a cream-colored background. The posterior surface of the thigh is mottled interleaved with cream-colored bars, forming a striped pattern (like the holotype) or with cream-colored large irregular-shaped spots surrounded by a mottled background. Female specimens are much larger than male specimens (SVL 31.1–34.6 mm, n = 3; 22.9–25.2 mm, n = 5, respectively). Variation in SVL and body proportions is given in Table 4.

Etymology: "Colibri" means hummingbird and is originally an Arawak (native people who lived on Haiti and other Caribbean islands) word. The word was adopted by many other languages, including Portuguese. The name is an allusion to the type locality of the new species, the municipality of Santa Teresa, which is known as "doce terra dos colibris" (sweet land of the hummingbirds). Santa Teresa is known as sweet land of the hummingbirds not only because of their abundance in the city, but also because of the Brazilian ornithologist Augusto Ruschi, who lived in Santa Teresa and dedicated his scientific life to the study of these little Neotropical birds. The name is used here as a noun in apposition.

Advertisement call: The advertisement call (ten calls of six males; Table 7; Fig. 6C) is emitted sporadically and is composed of 40–53 notes ($\overline{X}$ = 48.40 ± 3.86) emitted at regular intervals. The call begins with low energy notes, which increase in energy over time, until reaching a peak almost at the end of the call. Usually, the last two to five notes have notably less energy than the one before, and a decrease of energy is notable at the end of the call. The call rise time is 53–89% ($\overline{X}$ = 65.52 ± 12.34), and the dominant frequency is 2.67–2.84 kHz ($\overline{X}$ = 2.76 ± 0.05). Call duration is 0.90 to 1.20 s ($\overline{X}$ = 1.11 ± 0.09), and the note (repetition) rate is 41.30–44.82 notes per second ($\overline{X}$ = 43.54 ± 1.48). The note rate either accelerates or decelerates at the end of the call, and the note rate acceleration is −15 to 33% ($\overline{X}$ = 4.19 ± 13.70).

Territorial call: The territorial call (19 calls of two males; Table 7; Fig. 6D) has a similar structure to the advertisement call, but only the last note has notably less energy than the note before. In some calls the energy difference between the last and the penultimate note was not striking. The call rise time is 5–92% ($\overline{X}$ = 66.21 ± 28.35) and the dominant frequency is 2.63–2.89 kHz ($\overline{X}$ = 2.75 ± 0.09). Call duration is 0.17–0.51 s ($\overline{X}$ = 0.23 ± 0.11) and the note (repetition) rate is 44.44–48.78 notes per second ($\overline{X}$ = 46.35 ± 1.24). The note rate either accelerates or decelerates at the end of the call, and the note rate acceleration is −19 to 2% ($\overline{X}$ = −6.92 ± 7.46).

Comparison with other species: Finger I smaller than Finger II distinguishes *I. colibri* sp. nov. from members of the *I. guentheri*, *I. parva*, and *I verrucosa* series and from *I. manezinho* (Finger I approximately the same size as Finger II in these species; Garcia, 1996; Hedges et al., 2008). Expanded tips of fingers II–IV and large truncated discs of fingers III and IV distinguish *I. colibri* sp. nov. from members of the *I. parva* series, *I. nanahallux* (tips of fingers not expanded in these species; Hedges et al., 2008; Brusquetti et al., 2013), and members of the *I. verrucosa* series (disks small or moderate sized in these species; Hedges et al., 2008; Canedo et al., 2012). The large, conspicuous, glandular-appearing nuptial pad differentiates *I. colibri* sp. nov. from *I. manezinho*, *I. sambaqui*, *I. nanahallux*, and the members of the *I. lactea* (minute nuptial pad in *I. randorum;* translucent in *I.* nigriventris and *I. vizottoi*; reduced to some white granules in *I. holti* absent in *I. melanopygia* and *I. spanios;* unknown in other species; Heyer, 1985; Hedges et al., 2008; Targino and Carvalho-e-Silva, 2008; Berneck et al., 2013) and *I. verrucosa* series (except for *I. surda*; faint, translucent nuptial pad in *I. karst*; absent in other species; Hedges et al., 2008; Canedo et al., 2010, 2012). The mask-like stripe starting at the tip of the snout or the nostril, contouring the *canthus rostralis*, passing through the eye, contouring the dorsal portion of the tympanum and reaching the arm insertion distinguishes *I. colibri* sp. nov. from *I. manezinho*, *I. sambaqui*, and the members of the *I. guentheri*, *I. lactea*, and *I. verrucosa* series (mask-like stripe usually absent in these species; when present it does not pass through the eye). The smooth or finely tuberculate dorsum distinguishes *I. colibri* sp. nov. from *I. sambaqui* (rugose; Castanho and Haddad, 2000) and from the members of the *I. verrocusa* series (tuberculate in these species; Hedges et al., 2008; Canedo et al., 2010, 2012).

Its larger size distinguishes *I. colibri* sp. nov. (SVL of males 22.9–25.2 mm, n = 5; females 31.1–34.6 mm) from *I. venancioi* (SVL of males 15.7–22.3 mm, n = 31; female 24.1 mm, n = 1) and its smaller size distinguishes it from *I. hoehnei* (SVL of males 30.6–34.8 mm, n = 3; female 42.7 mm, n = 1) and *I. parnaso* sp. nov. (SVL of males 27.1–30.3 mm, n = 5; female 38.0 mm, n = 1). The medium-size foot and the small tibia (foot length/SVL = 0.52–0.60; tibia length/SVL = 0.56–0.62) differentiate *I. colibri* sp. nov. from *I. hoehnei* (foot length/SVL = 0.67–0.70; tibia length/SVL = 0.67–0.73). The mottled posterior surface of the thigh interleaved with cream-colored bars forming a striped pattern, or with cream-colored large irregular-shaped spots surrounded by a mottled background, differentiate *I. colibri* sp. nov. from *I. hoehnei* (posterior surface of the thigh mottled, forming small irregular spots in some specimens, spots cream-colored in life) and *I. venancioi* (posterior surface of thigh with cream-colored oval spots surrounded by a dark-brown background or with dark-brown slim bars on a cream-colored background; spots and background yellow to orange in life). The small fourth toe disk (fourth toe disk width/third finger disk width = 0.73–0.96) differentiates *I. colibri* sp. nov. from *I. parnaso* sp. nov. (fourth toe disk large; fourth toe disk width/third finger disk width = 1.00–1.09) and Finger I slightly smaller than Finger II (Finger I tip reaching the base of the disk of the Finger II) distinguishes *I. colibri* sp. nov. from *I. venancioi* (Finger I much smaller than Finger II; its size half to two thirds the size of Finger II).

The lower number of notes and higher dominant frequency of its advertisement call (40–53 notes per call; 2.67–2.84 kHz) differentiate *I. colibri* sp. nov. from *I. hoehnei* (59 notes per call; 1.90 kHz), and its higher number of notes in the advertisement call (40–53 notes per call) differentiates it from *I. parnaso* sp. nov. (18–29 notes per call). The higher note (repetition) rate differentiates *I. colibri* sp. nov. (41.30–44.82 notes per second) from *I. parnaso* sp. nov (16.55–21.17 notes per second) and *I. hoehnei* (35.85 notes per second).

Natural history notes: We found the species calling perched on leaves of ferns about 1.5–2.0 m in height. One male starts calling, followed by the other males. The following males start calling just before the previous male finishes his call, making a small overlap between the beginning and the end of the two calls. Some males also called alone, but we commonly heard two and three males calling together. The territorial call was not overlaid.

Geographic distribution: The species is currently known only from the municipality of Santa Teresa, state of Espírito Santo, Brazil.

Remarks: *Ischnocnema colibri* sp. nov. is the sister species of *Ischnocnema* aff. *venancioi* from the municipality of Cachoeiras de Macacu, state of Rio de Janeiro. We have only one specimen from Cachoeiras de Macacu, and despite its overall morphological resemblance to *I. colibri* sp. nov., we do not consider them conspecifics because it has a rounded snout in profile in dorsal view (acuminate in *I. colibri* sp. nov.) and the two species are genetically very distant (pairwise distance = 7.3% in partial 16S; Table 3). More specimens including molecular and acoustic data are paramount for the understanding of the taxonomic status of the population from Cachoeiras de Macacu.

4. Discussion

4.1. Phylogenetic relationships

Like other phylogenetic hypotheses, we recovered Brachycephalidae, *Brachycephalus*, and *Ischnocnema* as monophyletic (Hedges et al., 2008; Pyron and Wiens, 2011; Canedo and Haddad, 2012; Padial et al., 2014; Heinicke et al., 2017; Taucce et al., 2018). Despite using less species than other studies (six versus 14; Clemente-Carvalho et al., 2011; Padial et al., 2014), we also recovered the former *Psyllopryne didactyla* Izecksohn, 1971, nested among other species of *Brachycephalus*. These phylogenetic hypotheses show similar relationships, indicating that they are consistent and that probably they will not change over time.

Within the genus *Ischnocnema*, we recovered the former *I. guentheri* series (now *I. venancioi* plus *I. guentheri* series), the *I. lactea*, and *I. verrucosa* series as monophyletic, in accordance with previous studies (Canedo and Haddad, 2012; Taucce et al., 2018). The clade formed by *I.* cf. *manezinho* and *I. sambaqui*, currently unassigned to any species series, was also recovered by us and by previous phylogenetic hypotheses, confirming a strong relationship between these two species. However, the relationships between the two species and other species of *Ischnocnema* are uncertain. Canedo and Haddad (2012) and Taucce et al. (2018) recovered them as the sister group of the clade composed of *I. nanahallux* and the *I. verrucosa*, *I. parva*, *I. venancioi*, and *I. guentheri* series in their Bayesian inference and maximum likelihood analyses, the same relationship we found herein. Canedo and Haddad (2012) also presented a parsimony tree, in which they recover the *I. manezinho* clade as the sister group of the *I. lactea* series. Our parsimony tree shows a third phylogenetic position for the clade, but it is unsolved since it is poorly supported (Fig. S1).

The phylogenetic position of *I. nanahallux*, outside the *I. parva* series, is unprecedented. Taucce et al. (2018) were the first to test the phylogenetic position of *I. nanahallux* with a more comprehensive matrix, including more than one species of all *Ischnocnema* species series. They could not resolve its position, recovering it in a poorly supported *I. parva* series. The only genetic information available for *I. nanahallux* at the time was partial 16S tRNA on GenBank. Now we have more genetic information for the species (partial 12S, more parts of 16S, *RAG1*, and *Tyr*), and its position as the sister group of the *I. parva*, *I. venancioi*, and *I. guentheri* series was well-supported in all phylogenetic analyses that we performed (see results; Figs. 1 and S1).

4.2. Species-tree and time divergence

Our species-tree analysis yielded an overall similar tree to that of the other phylogenetic analyses, but with lack of resolution in the deepest relationships. The low resolution may be due to the lack of outgroups, but the species-tree topology, although without resolution in the deepest phylogenetic relationships, still corroborates the taxonomy of *Ischnocnema* proposed herein.

The time to the most recent common ancestor found for the genus *Ischnocnema* (48 Mya) was similar to the ones recovered in other studies (47 Mya, Heinicke et al., 2009), and it is similar to other Brachycephaloidea genera (*e.g. Haddadus*, *Craugastor*, and *Pristimantis*; Heinicke et al., 2009). However, it is older than other Neotropical frog genera, like *Thoropa* (27 Mya; Sabbag et al., 2018), *Leptodactylus* (35 Mya; Fouquet et al., 2013a), and *Adenomera* (21–25 Mya; Fouquet et al., 2013a, 2013b). The times to the most recent common ancestor within each of these Neotropical genera are more similar to the ones recovered herein for the *Ischnocnema* species series (38 Mya for the *I. verrucosa* series to 21 Mya for the *I. venancioi* series). The diversification times found within the *Ischnocnema* series date mostly to the Miocene, in accordance with those found for other South America amphibians (Rull, 2008). The clade encompassing all the *I.* aff. *parva* except for the one from Camacan, BA dates to 21.5 Mya, which is much older than the same clade in an other study (4 Mya; Gehara et al., 2017). Although we took the same clock rate for the mitochondrial partition (0.006 substitutions per site/Mya), this difference is probably due to differences in the matrix, since we have a species tree with more species (40 versus 7), and their study have more terminals for the *I. parva* series gene trees (65 versus 11). Another possible explanation for the time differences is that we used StarBEAST2 in our analysis, which implements a new species tree relaxed clock model (Ogilvie et al., 2017) compared to the previous version used by Gehara et al. (2017).The species described herein showed deep diversification times, the most recent for the split between *I. colibri* and *I.* aff. *venancioi*, 12 Mya. These splits are older than several other well stabilished species pairs (*e.g. I. abdita* and *I. bolbodactyla*) within *Ischnocnema*, showing that they are separately evolving metapopulation lineages and deserve to be described as new species.

4.3. Systematics within Ischnocnema

We increased the number of species of *Ischnocnema* to 37, with the description of two new species, and also raised the number of species series to five, with the description of the *I. venancioi* series. We created a new species series because the previous diagnostic morphological characters proposed for the *I. guentheri* series, including the *I. venancioi* series (see Hedges et al., 2008; Taucce et al., 2018), no longer apply. It is also a monophyletic and fully supported grouping in our three phylogenetic analyses, and bears unique morphological diagnostic features.

Three species are currently unassigned to any species series: *I. manezinho*, *I. nanahallux*, and *I. sambaqui*. *Ischnocnema manezinho* and *I. sambaqui* were previously assigned to the *I. lactea* series (Hedges et al., 2008) by morphological characters. Subsequently, Canedo and Haddad (2012) left these species unassigned to any species series due to molecular evidence; although they formed a fully supported clade, their position within *Ishnocnema* was uncertain. Padial et al. (2014) did not test the phylogenetic position of these species, but agreed with Canedo and Haddad (2012). Our results also recover the two species as sister taxa with strong support, and their phylogenetic position is similar in the Bayesian inference and in the maximum likelihood analyses but it is not supported in the maximum parsimony analysis. *Ischnocnema manezinho* was described from Florianópolis Island, Southern Brazil, but the sequence available for the species is from the municipality of São Bento do Sul, on the continent more than 150 km from the type locality. Despite strong evidence that *I. manezinho* and *I. sambaqui* form a clade and that they are not nested within any other species series, we find it more prudent to keep these species unassigned to species series until the phylogenetic position of *I. manezinho* from the type locality (Córrego Grande region, municipality of Florianópolis; Garcia, 1996) is tested.

Ischnocnema nanahallux was assigned to the *I. parva* species series at the time of its description based mainly on its morphological similarities, but also by molecular phylogenetic placement (Brusquetti et al., 2013). The authors' matrix included only five more *Ischnocnema* species (one species for each series except for the *I. guentheri* series, for which two were included) and *Brachycephalus didactylus*, but several *I. parva* specimens. Our results show a surprising phylogenetic position for *I. nanahallux*, as the sister group of the clade composed of the *I. parva*, *I. guentheri*, and *I. venancioi* series with strong support (Figs. 1 and S1). Because of the similar morphology between the members of the *I. parva* series and *I. nanahallux*, and because there are still several specimens with similar morphology in museum collections from places with DNA data not yet available, such as the states of Espírito Santo and Minas Gerais, Southeast Brazil (Taucce, P. P. G., unpublished data), we have chosen to take *I. nanahallux* out of the *I. parva* series and not to create a species series for it pending more genetic data available.

4.4. The nuptial pad

Most anurans have sexually dimorphic structures, such as vocal

sacs, vocal slits, and nuptial pads. These pads, present in male specimens, are glandular, keratinized, sometimes spiny structures typically on the first finger (Thomas et al., 1993; Luna et al., 2012). In the genus *Ischnocnema*, this character is an apparently glandular structure present on Finger I. Some species lack the pad, yet for others its presence is unknown. It can be large and conspicuous, as in the members of the *I. parva*, *I. guentheri*, and *I. venancioi* series, and also *I. surda* (member of the *I. verrucosa* series; Canedo et al., 2010; Brusquetti et al., 2013; Taucce et al., 2018; this study); minute, as in *I. randorum* (Heyer, 1985); faint and translucent, as in *I. karst*, *I. nigriventris*, and *I. vizottoi* (Martins and Haddad, 2010; Canedo et al., 2012; Berneck et al., 2013); and even reduced to some white granules as in *I. holti* (Targino and Carvalho-e-Silva, 2008). The nuptial pad is absent from the remaining species of the *I. verrucosa* series (Hedges et al., 2008), from *I. melanopygia* and *I. spanios*, of the *I. lactea* series (Heyer, 1985; Targino et al., 2009), from *I. manezinho* (Garcia, 1996), from *I. nanahallux* (Brusquetti et al., 2013), and from *I. sambaqui* (Castanho and Haddad, 2000).

Taucce et al. (2018) also recovered a grouping of the *I. parva* and the *I. guentheri* (including the *I. venancioi* series) species series. The authors also noted that the presence of a large, conspicuous, glandular-appearing nuptial pad on Finger I is a morphological feature that reinforces this grouping, despite its absence from *I. nanahallux*. According to our results, the presence of a large, conspicuous, glandular-appearing nuptial pad is a putative synapomorphy of the clade composed of the *I. parva*, *I. guentheri*, and *I. venancioi* series, which now does not include *I. nanahallux*. Outside this clade, this kind of nuptial pad is present only in *I. surda* (Canedo et al., 2010). This species was placed in the *I. verrucosa* series with its original description, but its phylogenetic position has never been tested. Due to the morphological variation of the nuptial pad in *Ischnocnema*, studies concerning morphological, histological, and chemical aspects of the pads are paramount to understanding the evolution of this character. It is also important to include more *Ischnocnema* species (like *I. surda* and *I. karst*) in future phylogenetic studies to assess the phylogenetic distribution of this character.

5. Conclusions

Our results demonstrate the monophyly of Brachycephalidae, *Brachycephalus*, and *Ischnocnema* with strong support. These relationships are recurrent in the literature and we consider them unlikely to change over time. The relationships within *Ischnocnema* are still weakly supported and controversial in some parts of the tree, and it is paramount to add more species and/or more genes to future analyses. The nuptial pad seems to be an important character in *Ischnocnema*, and future studies concerning morphological, histological, and chemical aspects of the pads allied with a strong phylogenetic hypothesis are necessary to understand the evolution of this character. The new *I. venancioi* series is a fully supported clade with several diagnostic morphological characters, and its relationships with the *I. parva* and the *I. guentheri* series are molecularly well-supported. A large, conspicuous, glandular-appearing nuptial pad is a putative synapomorphy for the clade formed by these species series. We raised the number of *Ischnocnema* species to 37 with the description of *I. parnaso* sp. nov. and *I. colibri* sp. nov. About 40% of these species were described over the past ten years, showing that there remains much taxonomic work to do for the genus.

Acknowledgments

We thank H. Q. Boudet, T. S. Soares (MBML), J. P. Pombal Jr (MNRJ), and K. de Queiroz (USNM) for making available material under their care. For support at the MNRJ we thank P. Pinna and M. W. Cardoso, and at USNM we thank A. Wynn. M. L. Lyra helped with laboratory procedures. We are grateful to Centro de Estudos de Insetos Sociais (CEIS; São Paulo State University [UNESP]) for allowing us the use of the molecular laboratory. A. A. Giaretta kindly shared call recordings and L. R. Malagoli kindly shared an *I. hoehnei* photograph. R. Collins helped with the package SPIDER. L. N. Barreto executed the drawings. E. R. Wild made English review. H. C. Costa helped with species names. This research was supported by resources supplied by the Center for Scientific Computing (NCC/GridUNESP) of UNESP and Cyberinfrastructure for Phylogenetic Research (CIPRES). P. P. G. T. thanks São Paulo Research Foundation (FAPESP), grant #2014/05772-4, Conselho Nacional de Desenvolvimento Científico e Tecnológico (CNPq), and Coordenação de Aperfeiçoamento de Pessoal de Nível Superior (CAPES) for the PhD fellowship and financial support, and Instituto Chico Mendes de Conservação da Biodiversidade (ICMBio) for collection permits (#42108). C. C. thanks Fundação Carlos Chagas Filho de Amparo à Pesquisa do Estado do Rio de Janeiro (FAPERJ), grant E-26/102.818/2011, for financial support. C. F. B. H. thanks FAPESP grant #2013/50741-7, FAPESP/Fundação Grupo Boticário de Proteção à Natureza grant #2014/50342-8, and CNPq for financial support. P. N. C. thanks Fundação Carlos Chagas Filho de Amparo à Pesquisa do Estado do Rio de janeiro (FAPERJ) for post-doctoral fellowships (processes E-26/201.760/2015, E-26/201.829/2015). L. O. D Thanks Conselho Nacional de Desenvolvimento Científico e Tecnológico (CNPq) for a PhD fellowship. L. O. D and P. N. C. thank Rede BioM.A. “Inventários: Padrões de diversidade, biogeografia e endemismo de espécies de mamíferos, aves, anfíbios, drosófilas e parasitos na Mata Atlântica” for financial and structural support (CNPq—process 457524/2012-0).

References

Berneck, B.V.M., Targino, M., Garcia, P.C.A., 2013. Rediscovery and re-description of *Ischnocnema nigriventris* (Lutz, 1925) (Anura: Terrarana: Brachycephalidae). Zootaxa 3694, 131–142. https://doi.org/10.11646/zootaxa.3694.2.2.

Bioacoustics Research Program, 2011. Raven Pro: Interactive Sound Analysis Software.

Bokermann, W.C.A., 1975. “1974”. Três espécies novas de *Eleutherodactylus* do sudeste da Bahia, Brasil (Anura, Leptodactylidae). Rev. Bras. Biol. 34, 11–18.

Bokermann, W.C.A., 1967. Una nueva espécie de *Eleutherodactylus* del sudeste brasileño (Amphibia, Leptodactylidae). Neotropica 13, 1–3.

Bokermann, W.C.A., 1965. A new *Eleutherodactylus* from Southeastern Brazil. Copeia 1965, 440–441. https://doi.org/10.2307/1440993.

Bossuyt, F., Milinkovitch, M.C., 2000. Convergent adaptive radiations in Madacascan and Asian ranid frogs reveal covariation between larval and adult traits. Proc. Natl. Acad. Sci. U. S. A. 97, 6585–6590. https://doi.org/10.1073/pnas.97.12.6585.

Bouckaert, R., Drummond, A.J., 2017. bModelTest: Bayesian phylogenetic site model averaging and model comparison. BMC Evol. Biol. 2017, 17–42. https://doi.org/10.1186/s12862-017-0890-6.

Bouckaert, R., Heled, J., Kühnert, D., Vaughan, T., Wu, C.-H., Xie, D., Suchard, M.A., Rambaut, A., Drummond, A.J., 2014. BEAST 2: a software platform for Bayesian evolutionary analysis. PLoS Comput. Biol. 10, e1003537. https://doi.org/10.1371/journal.pcbi.1003537.

Boulenger, G.A., 1888. V.— On some reptiles and batrachians from Iguarasse, Pernambuco. J. Nat. Hist. Ser. 6 2, 40–43. https://doi.org/10.1080/00222938809460873.

Brown, S.D.J., Collins, R.A., Boyer, S., Lefort, M.C., Malumbres-Olarte, J., Vink, C.J., Cruickshank, R.H., 2012. Spider: an R package for the analysis of species identity and evolution, with particular reference to DNA barcoding. Mol. Ecol. Resour. 12, 562–565. https://doi.org/10.1111/j.1755-0998.2011.03108.x.

Brusquetti, F., Thomé, M.T.C., Canedo, C., Condez, T.H., Haddad, C.F.B., 2013. A new species of *Ischnocnema parva* species series (Anura, Brachycephalidae) from northern state of Rio de Janeiro, Brazil. Herpetologica 69, 175–185. https://doi.org/10.1655/HERPETOLOGICA-D-12-00050.

Canedo, C., Haddad, C.F.B., 2012. Phylogenetic relationships within anuran clade Terrarana, with emphasis on the placement of Brazilian Atlantic rainforest frogs genus *Ischnocnema* (Anura: Brachycephalidae). Mol. Phylogenet. Evol. 65, 610–620. https://doi.org/10.1016/j.ympev.2012.07.016.

Canedo, C., Pimenta, B.V.S., 2010. New species of *Ischnocnema* (Anura, Brachycephalidae) from the Atlantic rainforest of the state of Espírito Santo. Brazil. South Am. J. Herpetol. 5, 199–206. https://doi.org/10.2994/057.005.0305.

Canedo, C., Pimenta, B.V.S., Leite, F.S.F., Caramaschi, U., 2010. New species of *Ischnocnema* (Anura: Brachycephalidae) from the state of Minas Gerais, Southeastern Brazil, with comments on the *I. verrucosa* Species Series. Copeia 2010, 629–634. https://doi.org/10.1643/CH-09-159.

Canedo, C., Targino, M., Leite, F.S.F., Haddad, C.F.B., 2012. A new species of *Ischnocnema* (Anura) from the São Francisco Basin Karst Region, Brazil. Herpetologica 68, 393–400. https://doi.org/10.1655/HERPETOLOGICA-D-11-00065.1.

Caramaschi, U., Canedo, C., 2006. Reassessment of the taxonomic status of the genera *Ischnocnema* Reinhardt and Lütken, 1862 and *Oreobates* Jiménez-de-la-Espada, 1872, with notes on the synonymy of *Leiuperus verrucosus* Reinhardt and Lütken, 1862 (Anura: Leptodactylidae). Zootaxa 1116, 43–54.

Caramaschi, U., Kisteumacher, G., 1989. "1988". A new species of *Eleutherodactylus* (Anura : Leptodactylidae) from Minas Gerais, Southeastern Brazil. Herpetologica 44, 423–426.
Castanho, L.M., Haddad, C.F.B., 2000. New species of *Eleutherodactylus* (Amphibia : Leptodactylidae) from Guaraqueçaba. Atlant. For. Brazil 2000, 777–781.
Clemente-Carvalho, R.B.G., Klaczko, J., Ivan Perez, S., Alves, A.C.R., Haddad, C.F.B., Dos Reis, S.F., 2011. Molecular phylogenetic relationships and phenotypic diversity in miniaturized toadlets, genus *Brachycephalus* (Amphibia: Anura: Brachycephalidae). Mol. Phylogenet. Evol. 61, 79–89. https://doi.org/10.1016/j.ympev.2011.05.017.
Cochran, D.M., 1948. A new subspecies of frog from Itatiaya. Brazil. Am. Museum Novit. 1375, 1–3.
Cocroft, R.B., Ryan, M.J., 1995. Patterns of advertisement call evolution in toads and chorus frogs. Anim. Behav. 49, 283–303.
Cope, E.D., 1862. On some new and little known American Anura. Proc. Acad. Nat. Sci. Philadelphia 14, 151 151–159 + 594.
Duellman, W.E., Lehr, E., 2009. Terrestrial-breeding frogs (Strabomantidae) in Peru. Natur und Tier - Verlag GmbH, Münster, Germany.
Dumeril, A.M.C., Bibron, G., 1841. Erpétologie générale ou histoire naturelle complète des reptiles. Tome huitième. Librarie Enclyclopedique de Roret, Paris.
Feller, A.E., Hedges, S.B., 1998. Molecular evidence for the early history of living amphibians. Mol. Phylogenet. Evol. 9, 509–516. https://doi.org/10.1006/mpev.1998.0500.
Fitzinger, L.J.F.J., 1826. Neue classification der reptilien nach ihren natürlichen verwandtschaften: nebst einer verwandtschafts-tafel und einem verzeichnisse der reptilien-sammlung des K. K. zoologischen museum's zu Wien, Isis Von Oken, J.G. Heubner, Wien: https://doi.org/10.5962/bhl.title.4683.
Fouquet, A., Blotto, B.L., Maronna, M.M., Verdade, V.K., Juncá, F.A., de Sá, R., Rodrigues, M.T., 2013a. Unexpected phylogenetic positions of the genera *Rupirana* and *Crossodactylodes* reveal insights into the biogeography and reproductive evolution of leptodactylid frogs. Mol. Phylogenet. Evol. 67, 445–457. https://doi.org/10.1016/j.ympev.2013.02.009.
Fouquet, A., Cassini, C.S., Haddad, C.F.B., Pech, N., Rodrigues, M.T., 2013b. Species delimitation, patterns of diversification and historical biogeography of the Neotropical frog genus *Adenomera* (Anura, Leptodactylidae). J. Biogeogr. 41, 855–870. https://doi.org/10.1111/jbi.12250.
Frost, D.R., 2018. Amphibian species of the world: an online reference [WWW Document]. Am. Museum Nat. Hist, New York, USA (accessed 1.15.18).
Garcia, P.C.A., 1996. Nova espécie de *Eleutherodactylus* Duméril and Bibron, 1891 (Amphibia, Anura, Leptodactylidae) do Estado de Santa Catarina, Brasil. Biociências 4, 57–68.
Gehara, M., Canedo, C., Haddad, C.F.B., Vences, M., 2013. From widespread to micro-endemic: molecular and acoustic analyses show that *Ischnocnema guentheri* (Amphibia: Brachycephalidae) is endemic to Rio de Janeiro. Brazil. Conserv. Genet. 14, 973–982. https://doi.org/10.1007/s10592-013-0488-5.
Gehara, M., Barth, A., Oliveira, E.F., Costa, M.A., Haddad, C.F., Vences, M., 2017. Model-based analyses reveal insular population diversification and cryptic frog species in the *Ischnocnema parva* complex in the Atlantic forest of Brazil. Mol. Phylogenet. Evol. 112, 68–78.
Gelman, A., Rubin, D.B., 1992. Inference from iterative simulation using multiple sequences. Stat. Sci. 7, 457–472.
Giaretta, A.A., Toffoli, D., Oliveira, L.E., 2007. A new species of *Ischnocnema* (Anura: Eleutherodactylinae) from open areas of the Cerrado Biome in southeastern Brazil. Zootaxa 51, 43–51.
Girard, C., 1853. Descriptions of new species of reptiles, collected by the U.S. Exploring Expedition, under the command of Capt. Charles Wilkes, U.S.N. Second part—including the species of batrachians, exotic to North America. Proc. Acad. Nat. Sci. Philadelphia 6, 420–424.
Goebel, A.M., Donnely, J.M., Atz, M.E., 1999. PCR primers and amplification methods for 12S ribosomal DNA, the control region, cytochrome oxidase I, and cytochrome b in bufonids and other frogs, and an overview of PCR primers which have amplified DNA in amphibians successfully. Mol. Phylogenet. Evol. 11, 163–199. https://doi.org/10.1006/mpev.1998.0538.
Goloboff, P.A., Catalano, S.A., 2016. TNT version 1.5, including a full implementation of phylogenetic morphometrics. Cladistics 32, 221–238. https://doi.org/10.1111/cla.12160.
Guindon, S., Dufayard, J.F., Lefort, V., Anisimova, M., Hordijk, W., Gascuel, O., 2010. New algorithms and methods to estimate maximum-likelihood phylogenies: assessing the performance of PhyML 3.0. Syst. Biol. 59, 307–321. https://doi.org/10.1093/sysbio/syq010.
Günther, A., 1858. On the systematic arrangement of the tailless batrachians and the structure of Rhinophrynus dorsalis. Proc. Zool. Soc. Lond. 26, 339–352.
Hedges, S.B., 1994. Molecular evidence for the origin of birds. Proc. Natl. Acad. Sci. U. S. A. 91, 2621–2624. https://doi.org/10.1073/pnas.91.7.2621.
Hedges, S.B., Duellman, W.E., Heinicke, M.P., 2008. New World direct-developing frogs (Anura: Terrarana): molecular phylogeny, classification, biogeography, and conservation. Zootaxa 1737, 1–182.
Heinicke, M.P., Duellman, W.E., Hedges, S.B., 2007. Major Caribbean and Central American frog faunas originated by ancient oceanic dispersal. Proc. Natl. Acad. Sci. U. S. A. 104, 10092–10097. https://doi.org/10.1073/pnas.0611051104.
Heinicke, M.P., Duellman, W.E., Trueb, L., Means, B., MacCulloch, R.D., Hedges, S.B., 2009. A new frog family (Anura: Terrarana) from South America and an expanded direct-developing clade revealed by molecular phylogeny. Zootaxa 2211, 1–35.
Heinicke, M.P., Lemmon, A.R., Moriarty-Lemmon, E., McGrath, K., Hedges, S.B., 2017. Phylogenomic support for evolutionary relationships of New World direct-developing frogs (Anura: Terraranae). Mol. Phylogenet. Evol. 118, 145–155. https://doi.org/10.1016/j.ympev.2017.09.021.
Hepp, F., Canedo, C., 2013. Advertisement and aggressive calls of *Ischnocnema oea* (Heyer, 1984) (Anura, Brachycephalidae). Zootaxa 3710, 197–199. https://doi.org/10.11646/zootaxa.3710.2.6.
Heyer, W.R., 1985. New species of frogs from Boracéia, São Paulo. Brazil. Proc. Biol. Soc. Washingt. 98, 657–671.
Heyer, W.R., 1984. Variation, systematics, and zoogeography of *Eleutherodactylus guentheri* and closely related species (Amphibia: Anura: Leptodactylidae). Smith Contr. Zool. 402, 15342. https://doi.org/10.5479/si.00810282.402.
Heyer, W.R., Rand, A.S., Cruz, C.A.G., Peixoto, O.L., Nelson, C.E., 1990. Frogs of Boracéia. Arq. Zool. 31, 235–410.
Hurvich, C., Tsai, C., 1989. Regression and time series model selection in small samples. Biometrika 76, 297–307. https://doi.org/10.1093/biomet/76.2.297.
Izecksohn, E., 1971. Nôvo gênero e nova espécie de Brachycephalidae do Estado do Rio de Janeiro. Bol. do Mus. Nac. Nov Série, Zool. 280, 1–12.
Jiménez de la Espada, M., 1870. Fauna neotropicalis species quaedam nondum cognitae. J. Sciências, Mathemáticas Phys. e Naturaes 3, 57–65.
Jiménez de la Espada, M., 1872. Nuevos batrácios Americanos. Anales Soc. Esp. Hist. Nat. 1, 84–88.
Katoh, K., Standley, D.M., 2013. MAFFT multiple sequence alignment software version 7: improvements in performance and usability. Mol. Biol. Evol. 30, 772–780. https://doi.org/10.1093/molbev/mst010.
Köhler, J., Jansen, M., Rodríguez, A., Kok, P.J.R., Toledo, L.F., Emmrich, M., Glaw, F., Haddad, C.F.B., Rödel, M.O., Vences, M., 2017. The use of bioacoustics in anuran taxonomy: theory, terminology, methods and recommendations for best practice. Zootaxa.
Kwet, A., Solé, M., 2005. Validation of *Hylodes henselii* Peters, 1870, from Southern Brazil and description of acoustic variation in *Eleutherodactylus guentheri* (Anura: Leptodactylidae). J. Herpetol. 39, 521–532. https://doi.org/10.1670/53-04A.1.
Lanfear, R., Frandsen, P.B., Wright, A.M., Senfeld, T., Calcott, B., 2017. Partitionfinder 2: new methods for selecting partitioned models of evolution for molecular and morphological phylogenetic analyses. Mol. Biol. Evol. 34, 772–773. https://doi.org/10.1093/molbev/msw260.
Langone, J.A., Segalla, M.V., 1996. Una nueva especie de *Eleutherodactylus* del Estado de Paraná, Brasil. Comun. Zool. del Mus. Hist. Nat. Montevideo 12, 1–5.
Ligges, U., Krey, S., Mersman, O., Schnackenberg, S., 2013. tuneR: analysis of music. URL: http://r-forge.r-project.org/projects/tuner/.
Luna, M.C., Taboada, C., Baêta, D., Faivovich, J., 2012. Structural diversity of nuptial pads in Phyllomedusinae (Amphibia: Anura: Hylidae). J. Morphol. 273, 712–724. https://doi.org/10.1002/jmor.20016.
Lutz, A., 1925. Batraciens du Brésil. Comptes Rendus Mémoires Hebd. des Séances la Société Biol. des ses. Fil. 22, 211–214.
Lutz, B., 1974. *Eleutherodactylus gualteri*, a new species from the Organ Mountains of Brazil. J. Herpetol. 8, 293–295. https://doi.org/10.2307/1562897.
Lutz, B., 1958. Anfíbios novos e raros das serras costeiras do Brasil: *Eleutherodactylus venancioi* n.sp., *E. hoehnei* n.sp., *Holoaden bradei* n.sp. e *H. lüderwaldti* Mir. Rib., 1920. Mem. Inst. Oswaldo Cruz 56, 372–389. https://doi.org/10.1590/S0074-02761958000200002.
Lynch, J.D., 1976. The species groups of South American frogs of the genus *Eleutherodactylus* (Leptodactylidae). Occas. Pap. Museum Nat. Hist. Univ. Kansas 61, 1–24.
Lynch, J.D., Duellman, W.E., 1997. Frogs of the genus *Eleutherodactylus* in western Ecuador biogeography. Spec. Publ. Nat. Hist. Museum Univ. Kansas 23, 1–236.
Lyra, M.L., Haddad, C.F.B., de Azeredo-Espin, A.M.L., 2017. Meeting the challenge of DNA barcoding Neotropical amphibians: polymerase chain reaction optimization and new COI primers. Mol. Ecol. Resour. 17, 966–980. https://doi.org/10.1111/1755-0998.12648.
Maniatis, T., Fritsch, E.F., Sambrook, J., 1982. Molecular cloning: a laboratory manual. Cold Spring Harbour Laboratory, New York.
Martins, I.A., Haddad, C.F.B., 2010. A new species of *Ischnocnema* from highlands of the Atlantic forest, Southeastern Brazil (Terrarana, Brachycephalidae). Zootaxa 65, 55–65.
Miranda-Ribeiro, A., 1937. Alguns batrachios novos das colleçções do Museo Nacional. O Campo 8, 66–69.
Miranda-Ribeiro, A., 1926. Notas para servirem ao estudo dos Gymnobatrachios (Anura) brasileiros. Arq. do Mus. Nac. 27, 1–227.
Miranda-Ribeiro, A., 1923. *Basanitia lactea* (Um novo batracchio das collecções do Museu Paulista). Rev. do Mus. Paul. 13, 851–852.
Ogilvie, H.A., Bouckaert, R., Drummond, A.J., 2017. StarBEAST2 brings faster species tree inference and accurate estimates of substitution rates. Mol. Biol. Evol. 34, 2101–2114. https://doi.org/10.1093/molbev/msx126.
Oliveira, L.E., Oliveira, R.M.C., Giaretta, A.A., 2008. *Ischnocnema hoehnei* (Hoehnei's Robber Frog). Advertisement call. Herpetol. Rev. 39, 207–208.
Padial, J.M., Castroviejo-Fisher, S., Köhler, J., Domic, E., De la Riva, I., 2007. Systematics of the *Eleutherodactylus fraudator* species group (Anura : Brachycephalidae). Herpetol. Monogr. 21, 213–240. https://doi.org/10.1655/06-007.1.
Padial, J.M., Grant, T., Frost, D.R., 2014. Molecular systematics of terraranas (Anura: Brachycephaloidea) with an assessment of the effects of alignment and optimality criteria. Zootaxa 3825, 1–132. https://doi.org/10.11646/zootaxa.3825.1.1.
Padial, J.M., Reichle, S., Riva, I. De, Padial, J.M., Riva, I.D.E.L.a., 2005. New species of *Ischnocnema* (Anura: Leptodactylidae) from the Andes of Bolivia. J. Herpetol. 39, 186–191.
Palumbi, S.R., Martin, A.P., Kessing, B.D., McMillan, W.O., 1991. Detecting population structure using mitochondrial DNA. In: Hoelzel, A.R. (Ed.), Genetic Ecology of Whales and Dolphins. International Whaling Comission, Cambridge, pp. 203–215.
Paradis, E., Claude, J., Strimmer, K., 2004. APE: Analyses of phylogenetics and evolution in R language. Bioinformatics 20, 289–290. https://doi.org/10.1093/bioinformatics/

btg412.
Peters, W.C.H., 1870. Über neue Amphien (*Hemidactylus*, *Urosaura*, *Tropdolepisma, Geophis, Uriechis, Scaphiophis, Hoplocephalus, Rana, Entomoglossus, Cystignathus, Hylodes, Arthroleptis, Phyllobates, Cophomantis*) des Königlich Zoologisch Museum. Monatsberichte der Königlichen Preuss. Akad. des Wissenschaften zu Berlin 1870, 641–652.
Pyron, R.A., Wiens, J.J., 2011. A large-scale phylogeny of Amphibia including over 2800 species, and a revised classification of extant frogs, salamanders, and caecilians. Mol. Phylogenet. Evol. 61, 543–583. https://doi.org/10.1016/j.ympev.2011.06.012.
Rambaut, A., 2014. FigTree. URL: http://tree.bio.ed.ac.uk/software/figtree/.
R Core Team, 2017. R: A language and Environment for Statistical Computing.
Reinhardt, J.T., Lütken, C.F., 1862. "1861". Bidrag til Kundskab om Brasiliens Padder og Krybdyr. Første Afdeling: Padderne og Øglerne. Vidensk. Meddelelser fra Dansk Naturhistorisk Foren. i Kjøbenhavn 2, 143–242.
Ronquist, F., Teslenko, M., Van Der Mark, P., Ayres, D.L., Darling, A., Höhna, S., Larget, B., Liu, L., Suchard, M.A., Huelsenbeck, J.P., 2012. Mrbayes 3.2: Efficient Bayesian phylogenetic inference and model choice across a large model space. Syst. Biol. 61, 539–542. https://doi.org/10.1093/sysbio/sys029.
Rull, V., 2008. Speciation timing and neotropical biodiversity: the Tertiary-Quaternary debate in the light of molecular phylogenetic evidence. Mol. Ecol. 17, 2722–2729. https://doi.org/10.1111/j.1365-294X.2008.03789.x.
Sabaj, M.H., 2016. Standard symbolic codes for institutional resource collections in herpetology and ichthyology: an online reference. Version 6.5 (16 August 2016). Electronically accessible at http://www.asih.org/, American Society of Ichthyologists and Herpetologists, Was 5, 802–832.
Sabbag, A.F., Lyra, M.L., Zamudio, K.R., Haddad, C.F.B., Feio, R.N., Leite, F.S.F., Gasparini, J.L., Brasileiro, C.A., 2018. Molecular phylogeny of Neotropical rock frogs reveals a long history of vicariant diversification in the Atlantic forest. Mol. Phylogenet. Evol. 122, 142–156.
Sazima, I., Cardoso, A.J., 1978. Uma espécie nova de *Eleutherodactylus* do sudeste Brasileiro (Amphibia, Anura, Leptodactylidae). Rev. Bras. Biol. 38, 921–925.
Spix, J.B. von, 1824. Animalia nova sive Species novae Testudinum et Ranarum quas in itinere per Brasiliam annis MDCCCXVII–MDCCCXX jussu et auspiciis Maximiliani Josephi I. F. S. Hübschmann, München.
Stamatakis, A., 2014. RAxML version 8: a tool for phylogenetic analysis and post-analysis of large phylogenies. Bioinformatics 30, 1312–1313. https://doi.org/10.1093/bioinformatics/btu033.
Steindachner, F., 1864. Batrachologische Mittheilungen. Verhandlungen des Zoologisch-Botanischen Vereins in Wien 14, 239–288.
Sueur, J., Aubin, T., Simonis, C., 2008. Seewave, a free modular tool for sound analysis and synthesis. Bioacoustics 18, 213–226. https://doi.org/10.1080/09524622.2008.9753600.
Targino, M., de Carvalho-e-Silva, S.P., 2008. Redescrição de *Ischnocnema holti* (Amphibia: Anura: Brachycephalidae). Rev. Bras. Zool. 25, 716–723. https://doi.org/10.1590/S0101-81752008000400017.
Targino, M., Costa, P.N., de Carvalho-e-Silva, S.P., 2009. Two new species of the *Ischnocnema lactea* Species Series from Itatiaia highlands, Southeastern Brazil (Amphibia, Anura, Brachycephalidae). South Am. J. Herpetol. 4, 139–150. https://doi.org/10.2994/057.004.0205.
Taucce, P.P.G., Canedo, C., Haddad, C.F.B., 2018. Two new species of *Ischnocnema* Reinhardt and Lütken, 1862 (Anura: Brachycephalidae) from Southeastern Brazil and their phylogenetic position within the *I. guentheri* species series. Herpetol. Monogr. 32, 1–21. https://doi.org/10.1655/HERPMONOGRAPHS-D-16-00014.1.
Thomas, E.O., Tsang, L., Licht, P., 1993. Comparative histochemistry of the sexually dimorphic skin glands of anuran Aamphibians. Copeia 1993, 133. https://doi.org/10.2307/1446304.
Titus, T.A., Larson, A., 1996. Molecular phylogenetics of desmognathine salamanders (Caudata: Plethodontidae): a reevaluation of evolution in ecology, life history, and morphology. Syst. Biol. 45, 451–472. https://doi.org/10.1093/sysbio/45.4.451.
Wilkinson, J.A., Matsui, M., Terachi, T., 1996. Geographic variation in a Japanese tree frog (*Rhacophorus arboreus*) revealed by PCR-aided restriction site analysis of mtDNA. J. Herpetol. 30, 418–423.